CELLULAR AND MOLECULAR STUDIES OF THE HUMAN PATHOGEN *CHLAMYDIA TRACHOMATIS*

BY

MALHAR DESAI

A THESIS SUBMITTED TO

THE SCHOOL OF GRADUATE STUDIES,

RUTGERS, THE STATE UNIVERSITY OF NEW JERSEY

IN PARTIAL FULFILLMENT OF THE REQUIREMENTS

FOR THE DEGREE OF

MASTER OF SCIENCE (M.S.)

GRADUATE PROGRAM IN

PHYSIOLOGY AND INTEGRATIVE BIOLOGY

WRITTEN UNDER THE DIRECTION OF

DR. HUIZHOU FAN

AND APPROVED BY

_____

_____

_____

_____

NEW BRUNSWICK, NEW JERSEY

MAY 2018

ABSTRACT OF THE THESIS

CELLULAR AND MOLECULAR STUDIES OF THE HUMAN PATHOGEN *CHLAMYDIA TRACHOMATIS*

by

MALHAR P. DESAI

Thesis Director:
Dr. Huizhou Fan

Chlamydia trachomatis is a gram-negative bacterium and human pathogen responsible for the most prevalent sexually transmitted infection in the world. Epidemiologic studies indicate that the number of new *C. trachomatis* infections reported in the US likely approaches as much as 0.5 per a population of 100 every year. This, when paired with the fact that all current forms of treatment for *C. trachomatis* infections have unintended side effects including harm to gut and vaginal microbiota, has compelled many biologists to look to further research on *C. trachomatis* in hopes of developing new antichlamydial agents. In this thesis, I review several projects involving *C. trachomatis* that provide a framework for understanding both the growth and the developmental cycle of *C. trachomatis.* Through a mixture of in-depth proteomics, transcriptomics, and *in vivo* assays, I present five overall conclusions: (i) *Lactobacilli*-derived lactic acid, at concentrations that are physiological in the cervicovaginal lumen, can disrupt the outer membrane complex of and inactivate *C. trachomatis*; (ii) immunoprecipitation of

chlamydial elementary bodies (EBs) using an antibody against a cell-surface protein of *C. trachomatis* is not an efficient method for purifying the bacterium; (iii) the growth of bacterial species that share significant sequence identity may not always be similar in media containing the same sera; (iv) the *Chlamydia*-specific transcription factor, GrgA, can stimulate transcription from promoters recognized by two different σ factors of *C. trachomatis* and has differential affinity for these two σ factors; (v) GrgA may associate with multiple subunits of the chlamydial RNA polymerase and, considering its role in transcription regulation and its specificity, may prove to be an excellent target for novel therapeutic agents against *C. trachomatis.*

ACKNOWLEDGEMENTS

First and foremost, I want to extend a very sincere note of gratitude to my mentor and program director, Dr. Huizhou Fan, who is also the principal investigator of our laboratory and a co-author on all studies performed in this report. Under his instruction, I was able to mature from a relative novice with little research background to an experienced scientist over the last 4 years. His knowledge and advice has helped me tackle many issues in my personal, academic, and research career, and provided me with enormous insight into "thinking as a researcher."

At the same time, I want to offer sincere and heartfelt apologies to my parents and my older brother for having to suffer silent disappointment from occasion to occasion. Entirely too busy performing research work over the last few years, I missed many a family lunch or dinner with them, and can only offer these 100 pages in compensation. Their remarkable warmth and affection towards me along with their financial support in all my years as a graduate student helped me significantly.

Next, I want to thank two of my fellow co-workers, Dr. Wurihan Wurihan and Dr. Huirong Zhang, for their collaborations and for keeping me company during my experiments both late at night and early in the day. Alongside this, I want to acknowledge and thank Dr. Rong Di, of the Department of Plant Biology at Rutgers University, for providing me with access to her BLItz machine, and for helping me design BLI experiments. I also want to make a special mention to two previous junior members of our laboratory, Mr. Alec Weber and Mr. Sangeevan Vellapan, for bringing brief, but necessary, moments of amusement and joy to a field that can often feel largely devoid of such.

As anybody who has conducted experiments might know, scientific research is rarely ever given to success on a first or even second try. Even with careful planning and a meticulous work-ethic, failure is always a possibility, which can make the process feel extremely disappointing and frustrating. At such times, taking a brief break from research – by going on vacation, engaging in a hobby, or simply having dinner – can be strangely reassuring and even constructive. Considering that I hardly ever have the motivation to engage in any of those activities in solitude, I want to acknowledge a few of my friends, mainly Ms. Megha Shah, Mr. Ankit Parikh, Ms. Jamie Shah, Mr. Don Vadakan, and Mr. Avinash Garlapati, for providing support to this research through their companionship without ever realizing.

Lastly, I want to acknowledge three senior faculty members at Rutgers University, namely Dr. Nancy Walworth, Dr. James Millonig, and Dr. Joseph Fondell, for taking the time to be a part of my thesis defense committee and for teaching me in graduate classes over the years. Dr. Fondell, in particular, was very mindful and supportive in helping me achieve my career goal.

TABLE OF CONTENTS

LIST OF ILLUSTRATIONS

LIST OF TABLES

LIST OF FIGURES

INTRODUCTION

Chlamydia trachomatis is an obligate intracellular bacterium and human pathogen that is responsible for the most prevalent sexually transmitted infection in the world. The World Health Organization (WHO) estimates that, out of the 350 million new cases of sexually transmitted infections that occur every year from common bacteria, an approximate 130 million new cases are caused by *C. trachomatis* alone [1]. Interestingly, the prevalence of *C. trachomatis* infection in females residing in the region of the Americas is estimated to be much higher (7.2%) than that of the global female population (4.5%) [1]. Considering that chlamydial infections in young women are often asymptomatic, it is likely that the number of reported cases that occur every year is an inaccurate descriptor for understanding the true prevalence of *C. trachomatis*. In fact, the Center for Disease Control (CDC) in the US predicts that the total number of new cases of chlamydial infections that occur every year could be ten times higher than the 1.5 million cases reported, making *C. trachomatis* a serious concern in the US [2, 3].

While susceptible to treatment with broad-spectrum antibiotics, a *C. trachomatis* infection can pose a severe challenge when left untreated. Upon moving to the upper genital tract, a *C. trachomatis* infection in women can result in pelvic inflammatory disease (PID), an infection of the uterus that could lead to damage of the fallopian tubes and eventual infertility. An untreated *C. trachomatis* infection can also give way to an ectopic pregnancy, a condition wherein the embryo attaches outside the uterus and causes the death of the resulting fetus. Furthermore, pregnant women with a *C. trachomatis* infection can experience other complications such as premature birth or abortion [4]. Alongside genital

infections, *C. trachomatis* can also introduce ocular infections in humans. In fact, *C. trachomatis* remains the leading cause of preventable blindness in most countries [5]. Considering these characteristics of *C. trachomatis* and the high prevalence of chlamydial infections in the US, the need to perform further research involving *C. trachomatis* is readily apparent. The fact that most of the antibiotics commonly used today for the treatment of a chlamydial infection tend to also cause harm to valuable members of the gut and vaginal microbiome furthers this notion as it highlights, above everything, the need to better understand chlamydial physiology and, through it, develop a better and more specific anti-chlamydial agent.

All species of *Chlamydia* share a unique, biphasic developmental cycle that involves two alternating cellular forms: the infectious elementary body (EB) and the noninfectious reticulate body (RB). Chlamydiae enter host cells as EBs and form vacuoles known as inclusions before differentiating into the more metabolically active RB. As RBs grow and expand, they eventually re-differentiate into EBs, which exit the host cell to infect other cells. Since the RB progression occurs in an asynchronous manner, the timeline of a typical *C. trachomatis* developmental cycle can have a wide range of 2 to 4 days. An illustration of a typical *C. trachomatis* cycle is provided on the next page (Ill. 0.1).

Transmission of *C. trachomatis*, as with *Neisseria gonorrhoeae* and the human immunodeficiency virus (HIV), occurs through sexual intercourse and shows sensitivity to many factors including the use of a contraceptive barrier, the existence of concurrent infections, and the pH of the cervicovaginal lumen in reproductive-age women [6-8]. While the former two are obvious determinants in the spread of any sexually transmitted

pathogen, the latter often comes as a notable revelation, and has only become evident in population-based studies carried out in the past 10 years [7].

In contrast to other species, culture of *C. trachomatis* has an added mandate; as an obligate intracellular organism, *C. trachomatis* requires a host cell line to grow inside. As a result, purification of *C. trachomatis* subsequent to culture and away from host cells has been routinely undertaken as a practice by chlamydial biologists. Culture of *C. trachomatis*, inside laboratories, requires the use of rich medium and the addition of growth factors essential for the host cells in the form of animal serum.

Considering that the cultivation of *C. trachomatis* seems well-characterized by most standards, *C. trachomatis* may seem, from a purely genomic standpoint, a relatively straightforward organism for study. However, the complex nature of the chlamydial developmental cycle suggests that all chlamydial species must undergo strong regulation throughout the developmental cycle in order to efficiently manage transitions between the two largely different cellular forms, a notion that has opened discussion about the possibility of temporal gene expression in *C. trachomatis.* As such, biologists working in both transcriptomic and genomic fields are likely to find the developmental cycle of *C. trachomatis* a fascinating topic for study.

In this thesis, I describe the attempts of our laboratory to navigate and understand the physiology and developmental cycle of *C. trachomatis*. Across the following pages, I recount five separate projects spanning several years and encompassing various aspects of chlamydial physiology, including the protein complex that forms its outer membrane (COMC), a transcription factor that regulates many of its genes (GrgA), and the two sigma

factors (σ^{28} and σ^{66}) of its RNA polymerase. I also touch upon the use of different sera in the growth of two closely related chlamydial species, review the benefits of specialized bioreactors for the growth of an anti-chlamydial antibody, and briefly describe attempts made to purify chlamydial EBs using an anti-chlamydial antibody. Using this work, our laboratory hopes to shed some light on pathways that regulate transcription and other processes inside chlamydia, and identify possible targets for the generation of highly specific anti-chlamydial drugs.
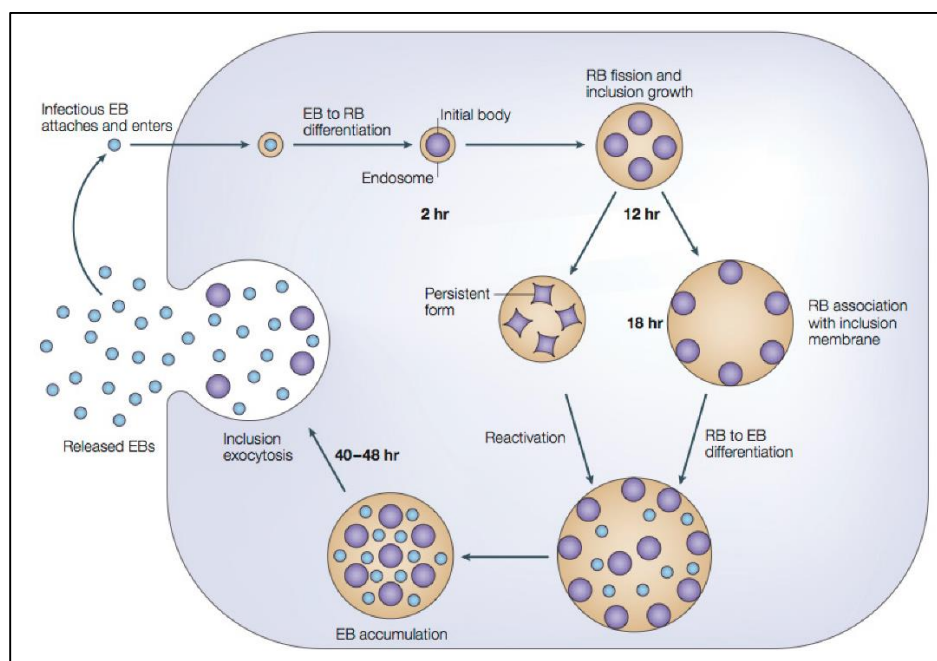
Ill. 0.1. An illustration of the life cycle of Chlamydia [9]. Between 0 and 4 h post-infection, an infectious EB attaches to and enters the host cell, and then differentiates into an RB. The RB then grows and divides by binary fission before eventually re-differentiating into an EB starting the midpoint of the developmental cycle. Finally, the EBs exit the host cell through either cell lysis or extrusion.

CHAPTER I

Disruption of *Chlamydia* Outer Membrane Complex by *Lactobacillus*-Derived Lactic Acid

ABSTRACT

Lactobacillus species that dominate the microbiome of the lower genital tract in reproductive women have been previously shown to inhibit colonization by other bacteria such as *Staphylococcus aureus* and *Escherichia coli.* However, the interaction between these *Lactobacilli* species and the human pathogen *Chlamydia trachomatis* has not been studied to any significant extent outside of our laboratory. While studies involving *S. aureus* and *E. coli* have largely attributed this ability of the *Lactobacilli* species to prevent and inhibit growth of invasive bacteria to their production of H_2O_2, we have previously shown that *Lactobacilli* mediate a similar inactivation of *C. trachomatis* infectivity through the production of lactic acid and not H_2O_2. Nonetheless, we have yet to identify a mechanism for this process. In this chapter, we propose a mechanism wherein lactic acid produced by *Lactobacilli* causes the disruption of the chlamydial outer membrane complex (COMC), leaving the contents of *C. trachomatis* exposed and susceptible to a low pH environment. We show evidence indicating that lactic acid reduces the disulfide bonds in the COMC in a pH- and concentration-dependent manner, and that it successfully achieves this reduction at concentrations and pH values that are physiologically found in the cervicovaginal lumen.

INTRODUCTION

In reproductive-age women, *C. trachomatis* infections are largely asymptomatic in the lower genital tract, and only develop into serious complications upon spreading to the upper genital tract [10]. Interestingly, the lower genital tract in reproductive-age women contains, amongst other non-pathogenic microbes, various *Lactobacillus* species that are thought to safeguard against colonization by pathogens. *Lactobacilli* isolated from the human vaginal tract have been previously shown to inhibit the growth of other pathogens such as *Staphylococcus aureus* and *Escherichia coli* through the production of H_2O_2 [11, 12]. Knowledge about the interaction between these same *Lactobacillus* species and the pathogen *C. trachomatis* is crucial to understanding and addressing the persistence of *C. trachomatis* infections across the world.

In the past, our laboratory has shown that *Lactobacilli* inactivate *C. trachomatis* infectivity through the production of lactic acid and not H_2O_2. We have also shown that the minimal H_2O_2 concentration required for any significant chlamydicidal activity is far greater than what is physiologically found in cervicovaginal secretions, and that the production of excess H_2O_2 coincides with reduced *Lactobacilli* growth and a sharp loss in chlamydicidal activity [13]. While there have been no instances of research detailing the interaction between *Lactobacilli* and *C. trachomatis* outside of our laboratory, many independent, population-based studies have linked a low cervicovaginal pH (between 3.5 and 4.0) with low Nugent scores (between 0-3) for bacterial vaginosis and low instances of reproductive tract infections in women [7, 8, 14]. This clinical observation, paired with our findings, suggests that lactic acid is, at the very least, directly involved in and partially responsible for the bactericidal ability of *Lactobacilli*.

Nonetheless, we have yet to identify a mechanism for how lactic acid produced by the *Lactobacilli* species inactivates *C. trachomatis*. Here I characterize a possible mechanism for the same by showing lactic acid-mediated reduction, and subsequent disruption, of the chlamydial outer membrane complex (COMC) *in vitro*. The COMC, which encases the EBs and protects against various forms of physical stress, consists mostly of cysteine-rich proteins, the most important of which is the major outer membrane protein (MOMP). Monomers of MOMP are linked by extensive disulfide bonding and form the backbone of the COMC [15].

In this chapter, I demonstrate that lactic acid, at concentrations and pH values that are considered physiological in the cervicovaginal lumen, can reduce the disulfide-bonds between the MOMP oligomers, resulting in the dissolution of the COMC and subsequent exposure of the contents of the EB to harsh conditions. Furthermore, I show that lactic acid performs this reduction in a pH- and concentration-dependent manner, which is consistent with our previous findings [13]. Together, these findings provide a groundwork for making sense of the clinical observations mentioned above, and highlight the importance of *Lactobacilli* colonization in maintaining a healthy reproductive tract.

RESULTS

Lactic acid reduces disulfide bonds in the COMC in a pH- and concentration-dependent manner. We treated COMC isolated from chlamydial EBs with lactic acid-containing buffers of different pH values and concentrations. At pH values below 4.0, lactic acid-containing buffers caused the reduction of disulfide bonds in the COMC and the release of MOMP (Fig. 1.1A). At a pH of 3.5 and concentrations close to those found in the cervicovaginal lumen (110 mM), lactic acid completely reduced the disulfide bonds between MOMP monomers in the COMC (Fig. 1.1B). This is consistent with our previous *in vivo* findings that show the complete inactivation of *C. trachomatis* upon treatment with *Lactobacilli*-conditioned media (LCM) that have pH values below 4.0 and lactic acid concentrations of 110 mM [13]. Furthermore, the lack of any significant effect on the COMC upon treatment with a lactic acid-containing buffer of pH 7.0 is also in agreement with our previous *in vivo* data that indicates that *C. trachomatis* viability remains largely unaffected when treated with LCM adjusted to pH 7.0 [13].
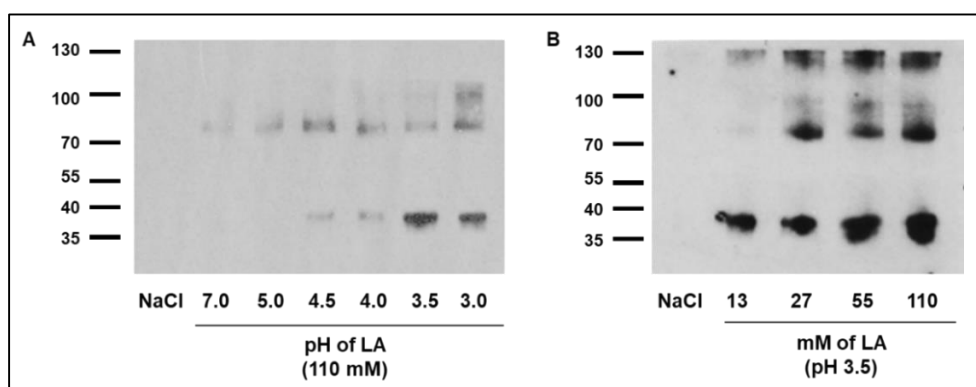
Figure 1.1. pH- and concentration-dependent reduction of COMC by LA. Western blots showing (A) pH- and (B) concentration-dependent reduction of reduction of *Chlamydia* outer membrane complex (COMC) by lactic acid (LA). Note that the native COMC resolves at greater than 180 kDa and therefore cannot be seen on the gel. Partially reduced COMC appears between 80 to 120 kDa. Completely reduced MOMP appears at 38 kDa. All Western blots shown here are detected using an anti-MOMP antibody.

At physiological concentration and pH, lactic acid reduces disulfide bonds in the COMC with a comparable efficiency as two commonly used reducing agents (DTT and TCEP). We treated COMC isolated from chlamydial EBs with lactic acid-containing buffers of different pH values. We also treated isolated COMC with one of two reducing agents, dithiothreitol (DTT) and tris(2-carboxyethyl) phosphine (TCEP), at concentrations that are commonly found in sample buffers used for SDS-PAGE in order to demonstrate the efficiency of reduction of COMC by lactic acid. At pH values below 4.5, lactic acid-containing buffers caused disulfide bond reduction in the COMC to a comparable extent as a buffer containing DTT or TCEP (Fig. 1.2). In fact, lactic acid may further denature other proteins in the COMC, as evident from bands lower than 38 kDa (Fig 1.2A).
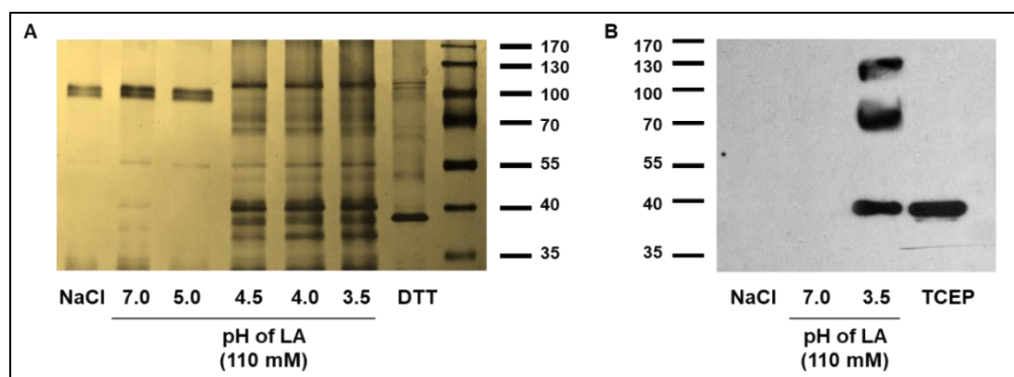
Figure 1.2. Reduction of isolated COMC by LA, DTT, and TCEP. Silver stain showing pH-dependent reduction of COMC by LA as well as reduction of COMC by 50 mM of DTT at pH 7.0 (A) and Western blot showing reduction of COMC by LA at pH 3.5 as well as reduction of COMC by 50 mM TCEP at pH 7.0 (B). Note that the native COMC resolves at greater than 180 kDa and therefore cannot be seen on the gel in its native form. On the gel, completely reduced MOMP appears at 38 kDa. Other completely reduced cysteine-rich proteins of the COMC can also be seen between 35-43 kDa.

At concentrations similar to lactic acid, two other organic acids (formic acid and acetic acid) can successfully reduce disulfide bonds in the COMC. We treated COMC isolated from chlamydial EBs with buffers containing 110 mM of one of three other acids (formic acid, acetic acid, and hydrochloric acid) at pH 3.5 and 4.0. Like lactic acid, the other two organic acids with strong buffering capacity (formic acid and acetic acid) were able to completely reduce the COMC at both pH 3.5 and 4.0 (Fig. 1.3). However, hydrochloric acid, which lacks any meaningful buffering capacity despite being a strong acid, was unable to reduce COMC to any extent. These findings are consistent with our previous *in vivo* data [13].
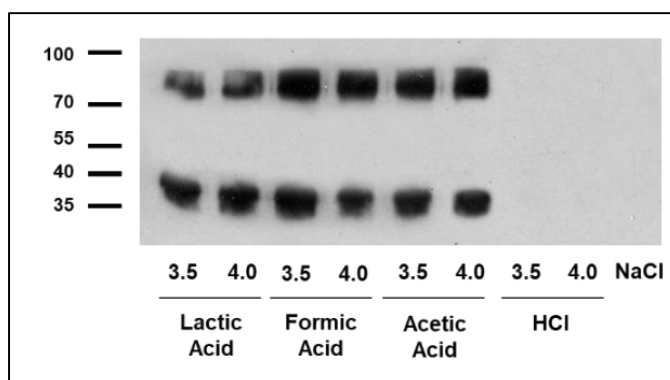
Figure 1.3. LA, FA, and AA can reduce COMC. Western blot showing reduction of reduction of *Chlamydia* outer membrane complex (COMC) by lactic acid, formic acid, and acetic acid. Hydrochloric acid (HCl) is unable to reduce COMC. Note that the native COMC resolves at greater than 180 kDa and therefore cannot be seen on the gel in its native form. Partially reduced portions of the COMC appear between 80 to 120 kDa. Completely reduced MOMP appears at 38 kDa. Western blot shown here is detected using an anti-MOMP antibody.

DISCUSSION

While the benefits of *Lactobacillus* colonization in the gastrointestinal (GI) tract have been researched and covered in extensive detail in literature over the course of the 20th century [16-20], the full impact of *Lactobacillus* colonization in the genital tract of women is only recently starting to be uncovered. In the past, theories have suggested that *Lactobacillus* species could produce a combination of lactic acid, H_2O_2, and various microbial peptides to shield against the colonization of pathogenic bacteria in both the GI tract and the genital tract [11, 13, 21, 22]. Research performed in the last 20 years has shown that lactobacilli exert a significant amount of control over the complete microbial flora of the genital tract [11-13]. However, studies largely attribute the inactivation of pathogenic bacteria to H_2O_2 production by lactobacilli [11, 12], which severely undercuts the corresponding role of lactic acid in this process. Population-based studies have routinely drawn correlations between the reproductive well-being of women and the acidity of the cervicovaginal lumen [7, 8, 14], suggesting that there is, at the least, interplay between the presence of lactic acid and the health of the genital tract.

In a study published in 2014 [13], our laboratory detailed the interaction of these *Lactobacillus* species with the pathogen *C. trachomatis*, and showed that lactobacilli reduce the viability of chlamydial EBs through the production of lactic acid and not H_2O_2 (ref). In the same study, we suggested that the ability of lactic acid to inactivate *C. trachomatis* could be due to three explanations: (i) lactic acid could radically destabilize surface molecules on EBs that allow the EBs to attach and enter the host; (ii) lactic acid could somehow cause damage to the outer membrane complex of *C. trachomatis* (COMC) and expose the components of the EB to the extracellular environment, which might prove

to be too harsh for some proteins and subsequently denature them; and (iii) protons (H$^+$) could enter the EB and inactivate the various components of the cell. At the time, we theorized that all three explanations were likely and could occur concurrently, but did not provide any evidence to support these claims.

As such, I provide initial evidence here showing that lactic acid, without the help of H$_2$O$_2$, can successfully manage the reduction of disulfide bonds within the COMC and initiate the disruption of the COMC to allow for further damage to the EBs. Additionally, I demonstrate that lactic acid reduces the COMC in a pH- and concentration-dependent manner (Fig. 1.1 and 1.2), explaining both our *in vivo* own findings [13] and the clinical observation that women with healthy and disease-free reproductive tracts most often have a pH of 3.5 or lower in their cervicovaginal lumen. I further report that other weak organic acids with strong buffering capacities (such as formic acid, citric acid, and acetic acid) can reduce disulfide bonds in the COMC *in vitro* and inactivate EBs *in vivo,* but that a strong acid such as HCl, at similar concentrations, is unable to reduce disulfide bonds in the COMC *in vitro* or cause any significant inactivation of EBs *in vivo* (Fig. 1.3). Considering this data, we theorize that lactic acid and other organic acids likely trigger the death of the EB by initially disrupting its protective outer covering through reduction and subsequently allowing hydrogen ions to flood the EB instead of simply lowering the extracellular pH in the way that a strong acid such as HCl would. It is possible that DTT, which lacks any significant acidic or buffering activity, is also unable to achieve the bactericidal activity of lactic acid despite being able to reduce the COMC *in vitro* as it is unable to provide the hydrogen-ions that are required to disable the machinery of the EB.

At the time of our previous study, our laboratory highlighted the findings of another group, Mastromarino et al., which showed that *C. trachomatis* experienced decreased growth when cultured alongside lactobacilli [23]. Another studies performed two years after our study has shown that the *Lactobacillus* species, *L. crispatus,* can inhibit the infectivity of *C. trachomatis in vitro* [24]. Paired with our data, these findings imply that *Lactobacillus* species in the cervicovaginal region may be able to activate the innate defense system of host cells upon encountering pathogenic bacteria. It may, therefore, be useful to fully characterize the interaction between these *Lactobacillus* species and vaginal epithelia in the future, both in the absence and presence of pathogenic bacteria. Regardless of whether or not lactobacilli can trigger such responses, the strongly mutualistic nature of their interaction with their host suggests that this relationship must have evolved over generations as a form of symbiosis and may be fundamental to maintaining a healthy reproductive tract. As such, our findings on the lactic acid produced by these *Lactobacillus* species have strong implications for physicians and researchers looking to develop new prophylactic or therapeutic agents against pathogenic bacteria such as *C. trachomatis*.

MATERIALS AND METHODS

Reagents: Stocks of the mouse L929 fibrobrast cell line and the L2 serovar of *C. trachomatis* were purchased from ATCC. The DMEM (Dulbecco's Modified Eagle Medium) with high glucose (4.5 g/L) and 110 mg sodium pyruvate, fetal bovine serum (FBS), trypsin (10x stock), 99.9% lactic acid solution, DTT powder, sodium *N*-laurosyl sarcosine (Sarkosyl), and TCEP (tris(2-carboxyethyl)phosphine)) were purchased from Sigma Aldrich. The Silver Stain Kit was purchased from Thermo Fisher. The unpurified mouse anti-MOMP monoclonal antibody was a generous gift from Dr. Guangming Zhong. The goat anti-mouse HRP-conjugated secondary antibody (A4416) was purchased from Sigma Aldrich. Purified EBs and RBs were generated by Dr. Xiaofeng Bao using gradient centrifugation.

Isolation of COMC from *C. trachomatis*: The COMC was isolated as per protocol provided by Caldwell et al. [25] except for a few changes. Multiple 6 mm^2 dishes were seeded with L929 cells and infected with stocks of the L2 serovar of *C. trachomatis* at 90% confluency at an MOI of 3. At 16 h post-infection, the cells were harvested using a cell scraper, sonicated on ice, and centrifuged at low-speed (3000 RPM) to remove cell debris. The supernatant was collected and centrifuged again at high-speed (14000 RPM) to move the EBs and RBs to the pellet, at which point they were resuspended in 500 μL of 1x PBS (pH 7.4) containing 2% (wt/vol) sodium *N*-laurosyl sarcosine (Sarkosyl) and 1.5 mM EDTA. The suspension was then sonicated on ice for a brief period of time (1 second ON, 1 second OFF, 2 minutes total) under 35% amplitude, and incubated at 37 °C for 1 hour. The suspension was then centrifuged at 12000g for 10 minutes, and the supernatant was

discarded. The pellet was again resuspended in 500 µL of 1x PBS (pH 7.4) containing 2% (wt/vol) sodium *N*-laurosyl sarcosine (Sarkosyl) and 1.5 mM EDTA. Followed by 1 hour of incubation at 37 °C, the suspension was centrifuged at 12000g for 10 minutes and the pellet was resuspended in 500 µL of PBS (pH 7.4) containing 25 µg of DNase I and RNase A each. The mixture was allowed to incubate for 2 hours at 37 °C. After a brief spin at 12000g, the supernatant was discarded, and the pellet was resuspended in 500 µL of 1x PBS (pH 7.4). The suspension was then subjected to multiple cycles of sonication (1 second ON, 1 second OFF, 6 minutes total) and centrifuged at 12000g for 10 minutes. The supernatant was discarded and the pellet (or the Sarksosyl-insoluble fraction, containing the isolated COMC) was used for experiments or stored at -80 °C.

Reduction of COMC: To test pH-dependence, samples of isolated COMC were treated with lactic acid-containing buffers with pH values of 7.0, 5.0, 4.0, 3.5, and 3.0 and concentration of 110 mM for 30 minutes at 37 °C. As a control, a sample of isolated COMC was treated with 0.9% NaCl (saline) solution. To test concentration-dependence, samples of isolated COMC were treated with buffers containing 13.7, 27.5, 55, and 110 mM lactic acid for 30 minutes at 37 °C.

Gel Analysis: All samples treated with lactic acid-buffers were mixed with 4x SDS Laemmli Buffer (containing no reducing agent) and resolved on a 10% SDS-polyacrylamide gel. All proteins were detected by either silver staining (as per protocol from the kit) or Western blot using the mouse anti-MOMP monoclonal antibody followed by secondary staining with the goat anti-mouse HRP-conjugated antibody.

CHAPTER II

Generation of an Anti-Chlamydial IgG Using a CELLine Bioreactor for the Pulldown of *Chlamydia trachomatis*

ABSTRACT

The gram-negative bacterium *Chlamydia trachomatis* was first isolated and identified as the cause of ocular infection in humans over 100 years ago. However, research on *C. trachomatis* in the intervening years has been limited by the fact that, being an obligate intracellular organism, *C. trachomatis* is unable to demonstrate growth and functional activity outside of a host. For researchers wishing to study the components of *C. trachomatis* in isolation, this aspect of chlamydial physiology has posed a severe challenge as it necessitates the purification of its inclusion bodies away from host cells. In the past few years, many methods for the purification of chlamydial EBs have been devised and implemented to varying success, with gradient-centrifugation considered the current gold standard by most researchers. However, the use of this method entails a large amount of technical work on the part of the researcher. Moreover, this method generally takes up to 9-10 hours and results in the recovering of only 60-70% of chlamydial particles. In this chapter, I report on an attempt to remodel the entire purification process. I detail the generation of an antibody against a cell-surface protein (MOMP) found in *C. trachomatis* using a special apparatus called the CELLine Bioreactor and report on my efforts at pulling down chlamydial EBs through immunoprecipitation with this antibody.

INTRODUCTION

First isolated by the Chinese researcher, Tang fei-Fan, as the cause of trachoma in the 1950s, the human pathogen *Chlamydia trachomatis* was initially thought of as a virus in the early part of the 20th century due to the fact that *C. trachomatis* only pertained in living cells [26]. In fact, it was not until the identification of both DNA and RNA inside *C. trachomatis* in the 1960s that it was designated as a bacterium. Though largely forgotten in the intervening years, this change in classification from a virus to a bacterium continues to serve as an important reminder in the 21st century of the fact that *C. trachomatis* exists only as an obligate intracellular organism. As such, most research pertaining to *C. trachomatis* has to be performed inside of a eukaryotic host cell line such as L929 or HeLa. Unfortunately, the growth of *C. trachomatis* in host cells routinely leads to cross-contamination in downstream experiments between components of *C. trachomatis* and components of the host cells. Genomic, transcriptomic, and proteomic studies frequently report the contamination of *C. trachomatis* samples with components of the host cell, making the data difficult to interpret [27-31]. To alleviate this issue, many researchers have resorted to purifying chlamydial EBs using different methods, all of which show varying success.

The most common methods for *C. trachomatis* purification are filtration of EBs using a glass or polycarbonate filter, and "gradient centrifugation" of EBs away from host cells. The latter technique, first detailed by Howard et al. in 1974 [32] and subsequently revised by others [33], including most prominently by Caldwell et al. [25], remains the current gold-standard for purification of chlamydial EBs and has been performed using many different reagents including sucrose, Renografin-76, and Percoll [32-35]. However,

the use of this method by researchers comes at the expense of a large amount of technical work, including extremely meticulous pipetting, and the purchase of expensive reagents. Even still, this method only guarantees about 60-70% recovery of total chlamydia particles and can take up to 10 hours. Exposure of chlamydial cells in the purification media for hours may alter the physiological states, a particular concern for many types of studies. The identification of any alternative methods for the purification of chlamydial EBs and RBs, therefore, remains an important step in furthering the course of all chlamydial research.

Recently, researchers have successfully used anti-chlamydial LPS antibodies to purify chlamydiae from vaginal fluid for genome sequencing [36]. Whereas the chlamydia recovery rate of the LPS antibody is not known, the LPS antibody could pull LPS out of the chlamydial cells. Therefore, I explored purification of *C. trachomatis* using an antibody against the major outer membrane proteins (MOMP).

In order to pursue this, it is crucial to generate and make available a large amount of purified anti-MOMP antibody. However, the presence of nonspecific and contaminating IgGs in most commercially available sources of fetal bovine serum (FBS) makes cell-culture of hybridoma cell lines using traditional flasks unsuitable for this process. In recent years, the introduction of semi-permeable cellulose-acetate membranes in cell culture flasks such as the CELLine Bioreactor has made it possible to avoid this contamination by isolating the cells away from the media. Unlike traditional cell-culture flasks, the CELLine Bioreactor is capable of harboring up to 400 million cells at a time, and contains two separate compartments to hold the cells and the media, as shown below (Ill. 1.1). This allows the cells to undergo rapid gas exchange and optimal growth while remaining

contaminant-free, and makes the CELLine Bioreactor an ideal choice for growing antibodies from hybridoma cell lines.

I report on the ease and efficiency of using of a CELLine Bioreactor to grow a mouse hybridoma cell line (L2-1-5), and review the quality and quantity of monoclonal antibody that can be generated using this apparatus. I subsequently detail our attempts at pulling down chlamydial cells using this antibody.
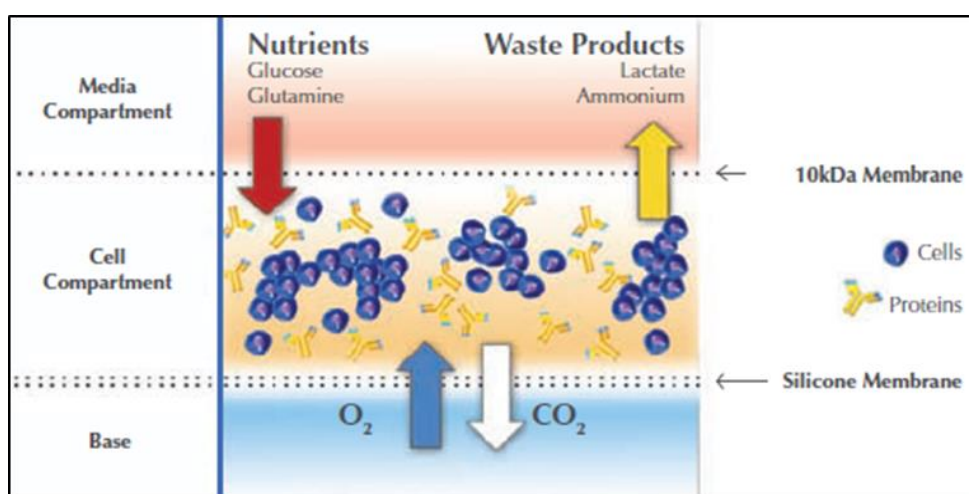
Ill. 2.1. An illustration provided by Wheaton Biologicals of the two compartments inside the CELLine Bioreactor. Gas exchange by cells occurs across the lower silicone membrane while nutrient exchange occurs across the upper cellulose-acetate biological membrane. Proteins greater than 10 kDa in size cannot pass across the biological membrane, restricting them to their original compartment.

RESULTS

The CELLine Bioreactor 1000 flask can be used to culture cells up to a population of 4 x 10^8 cells and can generate up to 600 μg of antibody/day. With a starting population of 5 x 10^6 cells grown from T75 flasks, we cultured a mouse hybridoma cell line capable of producing an anti-MOMP antibody in the serum-free compartment of a CELLine Bioreactor 1000 flask. Upon reaching a population of 4 x 10^8 cells, we harvested all cells from the CELLine Bioreactor, and re-inoculated the chamber with a second starting population of 7.5 x 10^7 cells. We harvested this culture once it reached a population of 3 x 10^8 cells. Table 2.1 below shows the daily growth of this mouse hybridoma cell line from the 2nd culture in the CELLine Bioreactor. A large amount of antibody can be generated and purified from a culture inside the CELLine Bioreactor. Using a part of the harvest from our 2nd CELLine culture, we purified approximately 654 μg of an anti-MOMP monoclonal antibody (Fig. 2.1) and conjugated it to magnetic Dynabeads. During immunostaining experiments, the anti-MOMP antibody was able to strongly stain inclusions of both the L2 and D serovars of *C. trachomatis* (data not shown).

Immunoprecipitation of chlamydial EBs from a sample of *C. trachomatis* using the L2-1-5 anti-MOMP antibody is not achievable in an efficient manner. We attempted the immuno-precipitation of a small portion (4%) of the total cell lysate from a T75 flask infected with *C. trachomatis* using 1% of our total Dynabeads-conjugated antibody. To our surprise, 2 μg of L2-1-5 anti-MOMP antibody was only able to immuno-precipitate roughly 1 μg of MOMP and therefore only a small amount of EBs (Fig. 2.2). Upon repeated trials, we obtained similar findings.

Table 2.1. Number of L2-1-5 hybridoma cells in CELLine culture. Data indicating estimated number of L2-1-5 hybridoma cells in culture in the CELLine 1000 flask over a 1-week period.

Day (Culture 2)	Number of Cells (x 10^7)
1	7.50
2	11.4
3	21.0
4	22.0
5	25.8
6	31.0
7	32.0
8	29.6
9	Harvest
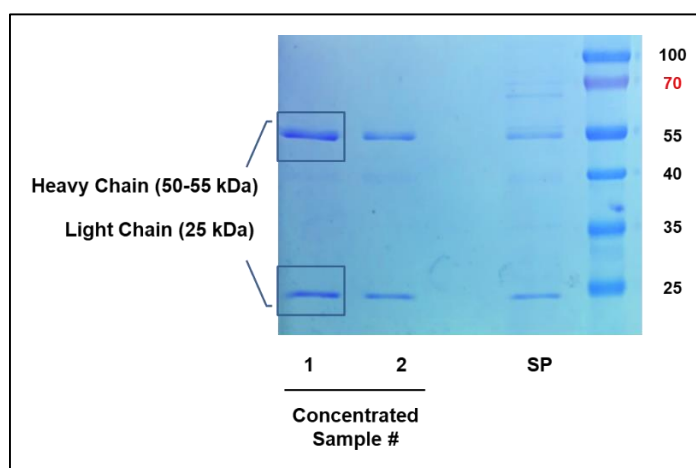
Figure. 2.1. Quality of affinity-purified L2-1-5 monoclonal antibody generated from CELLine culture. Coomassie-blue stain of a gel showing the purified heavy and light chains of L2-1-5 monoclonal antibody purified from a harvest of the 2nd CELLine culture, along with the heavy and light chains in the supernatant (SP) of cell suspension from the above CELLine culture.
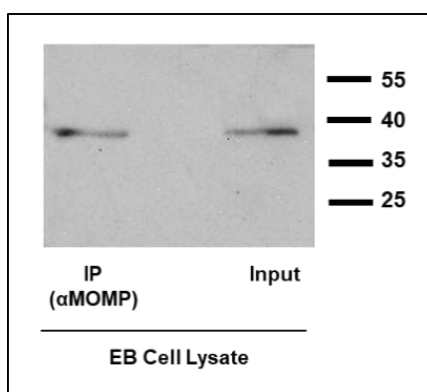
Figure 2.2. Pulldown of MOMP from a C. trachomatis sample using Dynabeads-conjugated anti-MOMP antibody. Western blot showing the immunoprecipitation result for a *C. trachomatis* sample precipitated with Dynabeads-conjugated anti-MOMP antibody and detected by a different mouse anti-MOMP antibody (MC22). Roughly 1% of the total cell lysate from a T75 flask infected with *C. trachomatis* was loaded onto the gel as an input. Note that reduced MOMP appears on the gel at 38 kDa.

DISCUSSION

As noted before, *C. trachomatis* remains a significant cause of concern both in the US and worldwide. Research involving *C. trachomatis* dates back to the mid-to-late 1900s and traces the evolutionary success and high prevalence of *C. trachomatis* to its two key biological characteristics. First, a *C. trachomatis* infection, despite being capable of leading to other complications, rarely presents with any significant symptoms in humans. As a result, *C. trachomatis* ensures its own survival by rapidly spreading across population of humans without severely affecting them in the manner than a deadlier pathogen such as HIV might. Secondly, *C. trachomatis* remains an obligate intracellular bacterium and, as such, is unable to reproduce or demonstrate any growth outside of its host, making *in vivo* research on *C. trachomatis* extremely difficult and limited to certain conditions. The latter of the two characteristics is especially challenging for researchers because the culturing of any bacterium alongside its host has the propensity to show cross-contamination between the two species, as is evident from many studies on *C. trachomatis* [27-30].

In recent years, researchers have circumvented this issue by resorting to purify chlamydial RBs and EBs away from their host cells before downstream analyses. A very common method for purification of intracellular bacteria such as *C. trachomatis* [32] and *Brucella abortus* [37] is to layer the bacteria on top of a discontinuous gradient before subjecting them to high-speed centrifugation, at which point the bacterial cells separate away from their host counterparts due to differences in density. This method, which has been refined over the years to improve its efficiency, is still a cause of inconvenience and worry to researchers for reasons that I have described before. Particularly, this method entails that the bacteria be subjected to a total of 6 hours of centrifugation with different

gradient mixtures, which makes this method an entirely unsuitable option for researchers wishing to study expression profiles of genes and proteins at specific times during the *C. trachomatis* developmental cycle. We ourselves have encountered both of these issues many times over the past few years and have had to change our research goals accordingly.

My findings in this report illustrate that immunoprecipitation of MOMP using the L2-1-5 antibody is inefficient and may require a large amounts of antibody to immuno-precipitate all MOMP present in the total cell lysate from a single T75 flask. While this makes the L2-1-5 antibody, at present, an inviable option for large-scale purification of EBs, it might be a feasible option for applications that require only a relatively small amount of chlamydiae.

Regardless of the overall success of such an experiment, evidence from studies performed by researchers with other bacterial cells suggests that the basis for performing this experiment may not be entirely unfounded. Immunoprecipitation of an entire protein complex using stationery matrix-affixed antibody molecules has been previously demonstrated to be successful in *Caulobacter crescentus* [38] and co-immunoprecipitation of protein complexes has been regularly performed in the past few years [39-42]. Furthermore, immunomagnetic separation (IMS), a routinely used technique in the isolation of pathogens from bodily fluids, cultured cells, and food samples, has been shown to efficiently separate cells from their host counterparts with the help of antibody-coupled Dynabeads [43-47]. However, these experiments, when performed in bacteria, have mostly been performed with species that are thought to have small cellular forms [48]. In the case of *C. trachomatis*, it is theoretically possible for multiple IgG molecules to bind a single EB due to its large size. In such a scenario, the binding capacity of the antibody and its

affinity to its antigen could exert a rather large influence on the outcome of the immuno-precipitation. As such, there is a possibility that, for purification of chlamydial cells (EB and/or RBs), antibodies against a low-abundance cell surface molecule may be more useful than an antibody for MOMP, which exists in high density on the cell surface. Alternatively, it is likely that immuno-precipitation across earlier time points with smaller-sized EBs and using different anti-MOMP antibodies may also yield better results.

Nevertheless, the findings in this report do carry some positive implications. First, my data (Table 2.1) (Fig. 2.1) illustrates that the CELLine Bioreactor remains an extremely powerful and efficient tool for the generation of antibodies from a hybridoma cell line. While the CELLine Bioreactor has been used for culturing eukaryotic cell lines [49, 50] and demonstrated to be more effective than ascites production in mice [51], the use of a CELLine Bioreactor for the generation of antibodies against *C. trachomatis*, or any other bacteria, has not been reported or demonstrated before this experiment. Secondly, my personal experience with the use of antibody-coupled Dynabeads indicates that the magnetic Dynabeads provide significant advantages over other types of stationary-matrices, many of which exhibit lower specificity, are harder to use, and have lower binding capacities for antibodies. When used in combination with a strong and potent antibody, magnetic Dynabeads could make the immunoprecipitation of proteins and their complexes from *C. trachomatis* a much simpler and straightforward process than traditional techniques, as we show in a later chapter.

As it stands, the development of a replacement method for the large scale purification of EBs and RBs than filtration or gradient centrifugation remains a yet to be realized task. The presence of contaminating host RNA in RNA-sequencing studies as

recent as 2017 [52] and even after gradient centrifugation [53] makes it critical that researchers devise an easier, more efficient, and less time-consuming method than the above two methods. Without an alternate approach, research on *C. trachomatis* is unlikely to escape the limitations it faces today.

MATERIALS AND METHODS

Reagents: The mouse L929 cell line was purchased from ATCC. The mouse L2-1-5 hybridoma cell line was a generous gift from Dr. Harlan D. Caldwell. Stocks of the L2 serovar of *C. trachomatis* were purchased from ATCC. The RPMI 1640 medium (containing 5g/L glucose and 4 mM L-glutamine), fetal bovine serum (FBS), and Wheaton CELLine 1000 flask were purchased from Sigma Aldrich. All cell culture-associated reagents (T75 flasks, 96 well-plates, and serological pipettes) were purchased from Greiner Bio-One. The Dynabeads Antibody Coupling Kit was purchased from Thermo Fisher. The anti-MOMP antibody used for detection on western blots (MC22) was generously provided by a Dr. Guangming Zhong.

CELLine Culture: Mouse L2-1-5 hybridoma cells were thawed from frozen stock and initially passaged in liquid media (RPMI 1640 containing 5 g/L glucose, 4 mM L-glutamine, and 10% FBS) in T75 flasks for 5-7 days with daily media change. After a sufficient number of cells were obtained (1.0×10^6 or more), the cells were harvested, centrifuged, and resuspended in 15 mL of RPMI 1640 containing 5 g/L glucose, 4 mM L-glutamine, and 10% FBS. Meanwhile, the outer "media" compartment of a Wheaton CELLine flask was subjected to an initial hydration using 10 mL of RPMI 1640 containing 5 g/L glucose, 4 mM L-glutamine, and 10% FBS for 5 minutes. The inner "cell" compartment was then seeded with the above cell suspension. Care was taken to ensure that no air bubbles were introduced into the cell compartment of the flask. Another 990 mL of RPMI containing 5 g/L glucose, 4 mM L-glutamine, and 10% FBS was then added to the media compartment. The number of cells in the cell compartment was approximated on a daily basis using a hematocytometer. In order to allow rapid growth of cells, the

medium from the outer compartment was changed at the end of every 72 hours, and a small aliquot of cell suspension was removed from the cell compartment to determine antibody titers on a biweekly basis. Once the cells had reached a population of 3×10^8 inside the cell compartment, the cell suspension was removed and centrifuged. The supernatant was collected, and stored for purification of IgG molecules. The pellet containing the cells was used to start a new liquid culture of T75 flasks.

Testing Antibody Titer: A 96-well plate was seeded with L929 cells and infected with stocks of the L2 serovar of *C. trachomatis* at 90% confluency. At 24 h post-infection, the cells were fixed using 100% methanol and washed three times with 1x PBS before being incubated with a blocking reagent (10% FBS) for 10 minutes. After the incubation, supernatant from the above L2-1-5 cell suspension was added at different dilutions to the wells of the 96 well-plate, and incubated at RT for 1 hour. As a control, a mouse anti-MoPn antibody (previously shown to stain cells of the L2 serovar) was added to wells that were not stained with the L2-1-5 mAb. After 3 washes with 1x PBS, the cells were incubated with a fluorescent secondary antibody (goat anti-mouse FITC, 1:1000) for 1 hour at RT. After 3 more washes with 1x PBS, the cells were visualized under a fluorescent microscope, and all antibody titers were obtained.

IgG Purification Using Protein A/G Agarose: Cells were harvested from the CELLine flask on day of harvest and centrifuged at 3000 RPM for 10 minutes. The supernatant was removed to a fresh tube, centrifuged again at 3000 RPM for 10 minutes, and filtered through a 0.2 um SFCA membrane filter with a syringe. The filtrate was then added to an Amicon Ultra-15 filter and concentrated using centrifugation at 14000g for 15 minutes. A gravity column was packed with Protein A/G agarose and washed with 20

column volumes (CV) of Protein A/G Wash Buffer or until the pH of the eluate reached 7.0. The filtrate from the above step was then loaded onto the column and incubated with the agarose for 30 minutes. After incubation, the pass-through was collected and the column was washed with 20 CVs of Protein A/G Wash Buffer. The antibody was eluted from the column in fractions using Protein A/G Elution Buffer and immediately neutralized using Protein A/G Neutralization Buffer. The quality of each fraction was assessed via SDS-PAGE followed by Coomassie-Blue staining. The best fractions were stored at -80 °C for later use.

Conjugation of L2-1-5 IgG to Dynabeads: A small amount of Dynabeads (5 mg per 50 μg of antibody) was weighed out and collected in a tube. The Dynabeads were then washed with 1 mL of C1 buffer and collected using a magnet. An appropriate amount of L21-5 IgG was added to the Dynabeads along with C1 and C2 buffers, and the mixture was incubated at 37 °C overnight on a Nutator. On the next day, a magnet was used to collect the Dynabeads. The pass-through was removed to another tube and put aside. The Dynabeads were then washed with 1 mL of HB followed by a wash with 1 mL of LB. Finally, the Dynabeads were given two washes of 1 mL each of SB and resuspended in 100 μL of SB per mg of beads to achieve a concentration of 1 mg of Dynabeads/mL. 0.01% NaN_3 was added to the Dynabeads to inhibit bacterial growth before being stored at 4 °C for long-term use. Note that a high-efficiency coupling protocol (with a ratio of 5 μg of antibody per 1 mg of Dynabeads) was utilized for the purpose of this experiment because an overabundance of antibody molecules on the Dynabeads is likely to cause overcrowding and be disadvantageous for the pulldown of a whole cell such as an EB. An alternate low-coupling protocol (with a ratio of 10 μg of antibody per 1 mg of Dynabeads) is possible.

CHAPTER III

Culture of *Chlamydia* Requires Testing of Serum on Individual Species

ABSTRACT

Fetal bovine serum (FBS) remains the most widely used growth medium supplement for *in vitro* culture of eukaryotic and bacterial cells. Newborn calf serum (NBCS), which is collected from calves of less than 14 days of age, is often used as a more cost-effective alternative to FBS for some cell lines. In this chapter, we demonstrate the effects of various bovine sera on the growth of two different chlamydial species (*C. trachomatis* and *C. muridarum*) that show significant sequence homology. While *C. trachomatis* cultures show no significant difference in infectivity when grown in DMEM containing 5% FBS or 5% NBCS from the same commercial source, *C. muridarum* cultures grown in DMEM containing 5% NBCS show an average of 20-fold reduction in infectivity rate compared to those grown in DMEM containing 5% FBS. Preliminary immunostaining experiments performed with chlamydial cultures indicate that high amounts of anti-chlamydial IgG molecules that specifically recognize *C. muridarum* but not *C. trachomatis* may be found in some sera and may serve as a possible explanation. Our findings indicate that bovine serum samples should be pre-screened, especially for researchers working with bacteria, at the species level.

INTRODUCTION

Cells in culture require a high amount of nutrients in order to grow and divide. Cell culture media is therefore routinely supplemented with animal serum, which serves as an effective source of these nutrients. Fetal bovine serum (FBS), which generally contains a large and diverse group of growth factors and a low amount of antibody molecules, has been a popular choice for researchers working with eukaryotic cell lines. However, the rising costs, availability, and ethical concerns associated with FBS have led some researchers to pursue using other alternatives to FBS, including newborn calf serum (NBCS) and horse serum (HS). While studies have previously shown NBCS to exhibit comparable or superior growth promoting capabilities to FBS in some eukaryotic cell lines [54], information about the effects of using NBCS with bacterial cultures has been limited and current understanding amongst researchers suggests that one must exercise caution when switching from FBS to NBCS.

Chlamydia trachomatis, an obligate intracellular bacterium, is the most prevalent species within the *Chlamydia* genus. The *Chlamydia* genus contains two other species that cause respiratory infections in humans (*C. pneumoniae* and *C. psittaci)* and six other species that cause infections in other animals (*C. muridarum, C. pecorum, C. suis, C. avium, C. felis,* and *C. gallinacea).* The most important of these is *C. muridarum*, which infects eukaryotes of the *Muridae* family, including mice, and shows significant sequence homology to *C. trachomatis*. Considering that humans cannot naturally contract infection through *C. muridarum*, it is routinely used in the laboratory as a replacement for studying *C. trachomatis*.

In this chapter, we characterize the growth of *C. trachomatis* and *C. muridarum* in a murine cell line with media containing different bovine sera. We demonstrate that, when tested after one passage in media containing either FBS and NBCS, *C. muridarum,* but not *C. trachomatis*, cultures show a marked loss in infectivity. We provide a possible explanation for these results by identifying the presence of IgG molecules against *C. muridarum* in our NBCS, and accordingly review the importance of performing growth tests for new sera at the species level in order to maintain the individual viability of each species.

RESULTS

***C. muridarum,* but not *C. trachomatis,* shows a significant decrease in infectivity rates across various sources of serum**. Cultures were grown in medium containing either FBS or NBCS and tested for infectivity after one passage. *C. trachomatis* cultures showed no significant change in infectivity rate when grown in media containing FBS or NBCS from Atlanta Biologicals (Fig 3.1). *C. muridarum* cultures, by comparison, showed a near 10-fold reduction in infectivity rate when grown with NBCS (Atlanta Biologicals) than with FBS (Sigma Aldrich, Atlanta Biologicals, or ATCC) (Fig. 3.1). Interestingly, both *C. muridarum* and *C. trachomatis* cultures showed a significant drop when cultured with FBS and animal serum complex (ASC) from Gemini Bio Products.

Detection of anti-*C. muridarum* antibody in NBCS. As a preliminary step towards further understanding this dissimilarity in growth using the different sera, all sera were tested for presence of anti-chlamydial antibodies by staining chlamydial inclusions with each serum followed by staining with a FITC-conjugated anti-bovine secondary IgG. When stained with NBCS, *C. muridarum* inclusions could be visibly detected under a fluorescent microscope, indicating that the NBCS sample contains anti-chlamydial antibodies that specifically recognize and bind to *C. muridarum*. Inclusions could not be detected for *C. muridarum* or *C. trachomatis* cultures stained with any other sera. Data for these immunostaining experiments is not shown in this chapter as microscopy photography was not possible due to moderate amounts of background staining of host cells from the sera.
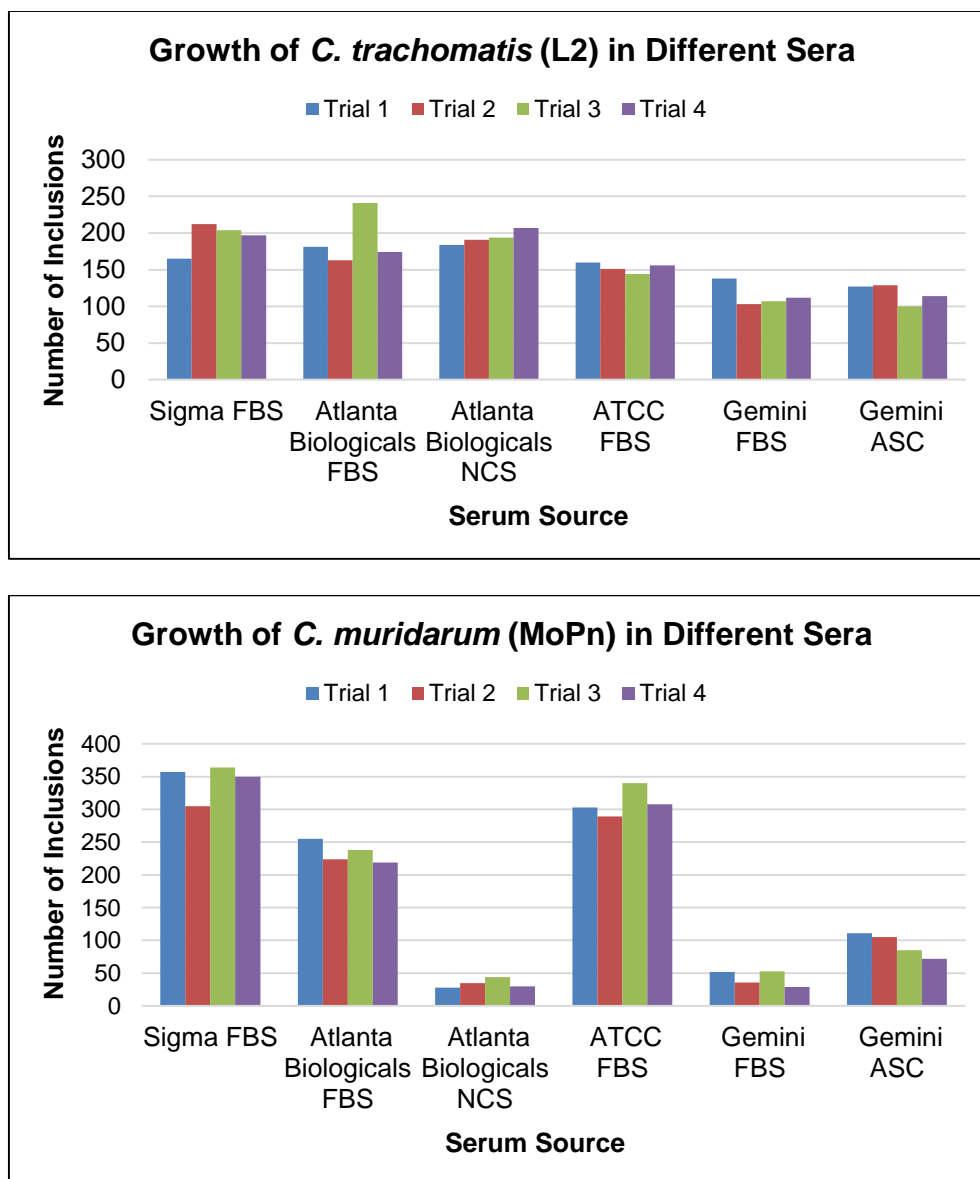
Figure 3.1. Growth of *C. trachomatis* **and** *C. muridarum* **in media containing various sera.** Bar-graph showing amount of chlamydial L2 inclusions (upper) and MoPn inclusions (lower) arising from cultures grown in media containing the indicated sera.

DISCUSSION

Theorized for hundreds of years, the culture of cells and tissues outside their natural environment was only first made possible in the early 1900s with the development of specific salt solutions and reagents. Since then, cell culture has become a staple of modern biological research, and has allowed for significant advancements in our understanding of humans and other species. The process itself has moved through changes and breakthroughs through the years with the advent of highly sterile and rich media options catered towards optimizing growth of cells. One such option is the use of a growth supplement such as animal serum, which contains many factors and proteins to help cells divide and proliferate.

As noted before, the most commonly used growth supplement in research today is fetal bovine serum (FBS), a component of blood from fetal cows that serves as a very diverse source of nutrients for growing cells. While its benefits in cell culture are clear and evident, the use of FBS has, in the years since its first discovery as a byproduct of the dairy industry, become a source of concern for some people for three reasons: first, the use of FBS has raised many ethical questions amongst researchers, and regularly been decried by animal rights groups over the years; secondly, FBS is often sold at very high price rates by commercial companies, and, with increasing demand, has seen an absurd 300% increase in price in the US since 2011 [54]; and, lastly, the large variation in composition across different sources, and even batches, of FBS has made it difficult for researchers to identify a single brand or type of FBS to use.

Many researchers working mainly with eukaryotic cell lines in the last 5 years have chosen to instead move to other source of serum such as newborn calf serum (NBCS) and animal serum complex (ASC), both of which are less expensive and more readily available than FBS. However, these so-called "FBS alternatives" are thought to carry a higher amount of antibodies and complement compared to FBS, making it important that researchers test these FBS alternatives with their cell lines prior to experiments. While this switch to FBS alternatives has been demonstrated to be effective in a study of 6 different eukaryotic cell lines [54], the use of FBS alternatives has not been studied with any bacteria to date. Authors of the aforementioned study note that, while the use of NBCS can be as comparable as FBS, there can be changes in cell morphology in some of the cell lines with the use of NBCS [54], suggesting that the effects of NBCS on the cells may be subtle.

We further this notion by showing dissimilar growth in two very similar intracellular bacterial species, *C. trachomatis* and *C. muridarum,* when cultured with NBCS. In spite of the fact that it shares significant sequence homology with *C. trachomatis*, *C. muridarum* shows a clear loss in infectivity (near 10-fold) after just one passage when cultured in media containing NBCS as compared to FBS from Sigma Aldrich (Fig. 3.1). Similarly, the use of ASC also entails a 5-fold reduction in infectivity of *C. muridarum* compared to FBS from Sigma Aldrich. Consistent with the idea that NBCS may carry more antibodies than FBS, we report the presence of IgG molecules against *C. muridarum* in NBCS but not any sources of FBS (as indicated before, data not shown). Furthermore, in keeping with the notion that FBS samples tend to show large variation based upon source, we document a respective 2- and 5-fold inconsistency in infectivity rates of *C. trachomatis* and *C. muridarum* when grown with different sources of FBS (Fig. 3.1). All together, these

findings indicate that the use of some sera can prove deleterious for the culture of some bacterial species after just one passage. In light of this data, we recommend to other researchers that the screening of any sera, with respect to its growth promoting ability in any cell line, be performed at the species level rather than at the genus level, where it is routinely performed, in order to correctly ascertain proper growth of individual species.

MATERIALS AND METHODS

Reagents and Cell Lines: L929, a mouse fibroblast cell line, was used as host for chlamydial infection. A clone of a *C. trachomatis* L2 strain, CPAF-deficient-Bu343, that contains two mutations in the ORF of the *CPAF* protein, and a *C. muridarum* strain, MoPn, were used to infect L929 cells. Dulbecco's Modified Eagle Medium (DMEM) containing high glucose (4.5 g/L) and sodium pyruvate (110 mg), gentamycin (10 mg/mL stock), and trypsin were purchased from Sigma Aldrich. The sera were purchased from several sources: fetal bovine serum was purchased from Sigma Aldrich (Canadian Origin), Atlanta Biologicals, ATCC, and Gemini, animal serum complex (ASC) was purchased from Gemini, and new-born calf serum (NBCS) was purchased from Atlanta Biologicals. The SPG buffer contained 220 mM sucrose, 10 mM sodium phosphate, and 0.50 mM L-glutamic acid.

Preparation of Media and Growth Sera: FBS, ASC, and NBCS from the various sources were thawed and subjected to heat-shock as suggested in original protocol. After heat-shock, 2.5 mL of serum was removed from each serum bottle, and added to a fresh 50 mL aliquot of DMEM. Thus, six total DMEM preparations were made, each containing 5% serum from one of the indicated sources: #1 (FBS, Sigma Aldrich), #2 (FBS, Atlanta Biologicals), #3 (FBS, ATCC), #4 (FBS, Gemini), #5 (ASC, Gemini), and #6 (NBCS, Atlanta Biologicals).

Growth Assay Using Different Sera: L929 cells were seeded onto a 6-well plate, and grown to 90% confluency in DMEM containing 5% FBS (Sigma Aldrich). Just prior to infection, all media was removed from each well, and replaced with one of the six

DMEM preparations (#1, 2, 3, 4, 5, or 6). All wells of the six-well plate were infected with the CPAF-deficient Bu343 strain. At 36 h post-infection, all media was removed, and was replaced with 100 μL of SPG buffer. The cells were then harvested using a cell scraper, and removed to six separate tubes. All tubes were then sonicated on ice at 35% amplitude (1 second ON, 1 second OFF, 10 seconds) and centrifuged at 3000 RPM for 10 minutes. The supernatant was collected from each tube, subject to serial dilution, and used for further infection. The same protocol was followed for the MoPn strain, with one notable change: the cells of the MoPn serovar were harvested at 30 h post-infection, instead of 36.

Immunostaining of Chlamydial Inclusions: A 96-well plate was seeded with L929 cells and infected at 90% confluency with harvests from the above L2 culture. All cells were subject to the same media conditions (DMEM containing 5% FBS, Sigma Aldrich). At 24 h post-infection, the cells were fixed using 100% methanol, and washed three times with 1x PBS before being incubated with a blocking reagent (10% FBS, Sigma Aldrich) for 10 minutes. After the incubation, the blocking agent was removed, and the cells were then incubated with a primary antibody (mouse anti-MOMP L2-1-5 monoclonal antibody, 1:1000) for 1 hour at RT. After three washes with 1x PBS, the cells were incubated with a fluorescent secondary antibody (goat anti-mouse FITC, 1:1000) for 1 hour at RT. After 3 more washes with 1x PBS, the cells were visualized under a fluorescent microscope, and all chlamydial inclusions were counted. The same protocol was followed for the MoPn strain, with two notable changes: the inclusions were fixed at 30 h post-infection, instead of 24, and stained using a different primary antibody (mouse anti-MoPn antibody, 1:1000).

Immunostaining of Chlamydial Inclusions Using Various Sera: A 96-well plate was seeded with L929 cells and infected with stocks of either the CPAF-deficient-Bu343 clone of *C. trachomatis* or the MoPn strain at 90% confluency. Several h post-infection (24 hours for the *C. trachomatis* strain, 30 hours for the *C. muridarum* strain), the cells were fixed using 100% methanol, and washed three times with 1x PBS before being incubated with a non-bovine blocking reagent (10% horse serum) for 10 minutes. After the incubation, the cells were incubated for 1 hour at RT with 1:1000, 1:500, 1:100, and 1:50 dilutions of the various FBS, ASC, or NBCS. As a control, a mouse anti-MoPn antibody (previously shown to stain cells of both serovars) was added to wells that were not incubated with the sera. After 3 washes with 1x PBS, the cells were incubated with a fluorescent secondary antibody (goat anti-bovine FITC, 1:1000, for the wells stained with FBS or NBCS, and goat anti-mouse FITC, 1:1000, for wells stained with the control antibody) for 1 hour at RT. After 3 more washes with 1x PBS, the cells were visualized under a fluorescent microscope, and staining of any chlamydial inclusions by antibodies present in the sera was determined.

CHAPTER IV

Biochemical Evidence for the Differential Regulation of σ^{66} and σ^{28}-Dependent Genes by GrgA in *Chlamydia trachomatis*

ABSTRACT

The proteome of *C. trachomatis* has roughly 900 members, of which most are only expressed according to temporal changes during the length of the chlamydial developmental cycle. Since most bacterial species, including *C. trachomatis*, rely upon transcriptional regulation to control expression, it is reasonable to assume that the actions of transcription factors carry significant importance for the overall organism, which in turn makes these transcription factors valuable to the study of *C. trachomatis*. We have previously identified a *Chlamydia*-specific transcription factor called GrgA that contacts the major σ factor of the chlamydial RNA polymerase (σ^{66}) in order to activate transcription *in vitro*. However, we have yet to characterize the interaction between GrgA and one of the other two σ factors in *C. trachomatis* (σ^{28} and σ^{54}). In this chapter, we provide evidence to show that GrgA binds σ^{28} and stimulates transcription activation from a σ^{28}-dependent promoter *in vitro*. Through a combination of pulldown assays and bio-layer interferometry (BLI), we then characterize the kinetics and relationship of the GrgA-σ^{66} and the GrgA-σ^{28} interactions to show that GrgA shows differential regulation of the two σ factors. Using these findings along with others, we establish a framework in this report to show that GrgA, as a highly essential protein that is utilized at multiple phases of the chlamydial developmental cycle, may be a suitable target for the derivation of novel therapeutics against *C. trachomatis.*

INTRODUCTION

As mentioned in previous chapters, all chlamydial species share a complex and unique development cycle given to alternation between two cellular life forms. Although microscopy experiments have detailed the morphological and phenotypical changes that take place during the progression of this developmental cycle [55-61], the genomic signals that prompt the conversion of one cellular form to another and the proliferation of RBs have not been fully identified. The detection of time-influenced changes in the gene expression of *C. trachomatis* in microarray studies over the years [62-66] has led researchers to classify genes into three broad categories based on their expression pattern: an early-stage period of 0 to 8 h post-infection, wherein the elementary body (EB) first enters the host cell and converts to a reticulate body (RB); a middle-stage period of 8 to 24 h post-infection, wherein the RB undergoes proliferation and division; and a late-stage period of 24 to 40 h post-infection, wherein the RBs differentiate back into the EBs. Since EBs and RBs tend to dominate at two different stages in the cell cycle, it is logical to assume that some genes are expressed only in EBs or only in RBs, a notion which is also supported by microarray studies [63, 66]. These two findings [63, 65, 66] indicate that regulation of gene expression at the transcriptional level is possibly the most important aspect of *C. trachomatis* governing its life cycle.

As with other gram-negative bacteria such as *Escherichia coli* [67], transcription in *C. trachomatis* is carried out by a multi-subunit RNA polymerase, comprised of two α subunits, a β subunit, and β' subunit [68]. However, unlike its *E. coli* counterpart, the chlamydial RNA polymerase has no known ω subunit. The chlamydial genome also encodes three sigma factors (σ^{28}, σ^{66}, and σ^{54}) that share substantial homology with that of

other bacteria [69-72]. These σ factors combine with the core-enzyme to form the fully functional RNA polymerase holoenzyme.

While the function and targets of σ^{54} remain largely a mystery [72], the other two σ factors have been well-studied in the past few years and genes under their control have been identified in multiple studies. The primary housekeeping σ factor encoded by chlamydia, σ^{66} is thought to direct transcription of most of the early and mid-late stage genes along with a few late genes [73, 74]. Many critical genes present in *C. trachomatis*, including the major outer membrane protein (MOMP), have been transcribed *in vitro* using a RNA polymerase holoenzyme containing σ^{66} [75]. On the other hand, σ^{28} is thought to predominantly control expression of stress-related and late stage genes [76, 77], including the gene *hctB* that encodes a protein thought to be involved in the conversion of the RB to the EB [78]. The differential regulation of these σ factors [62] and the genes under their promoter control by transcription factors is thought to have significant implication in allowing chlamydia to successfully carry out its developmental cycle. Considering that these two σ factors regulate genes involved in different parts of the cell cycle, it is crucial to characterize the interaction between them and any transcription factors that have the ability to regulate them.

We have previously [79] identified an important transcription factor in *C. trachomatis*, CTL0766, that we have named GrgA (General Regulator of Genes A). We have shown that GrgA, a 288-amino acid protein, binds both DNA and the chlamydial RNA polymerase, and that it regulates transcription of many chlamydial genes *in vitro* [79]. While conserved across most chlamydial species, GrgA has no known homolog in other bacteria or eukaryotes, suggesting that its role in transcription is integral to the unique

developmental cycle of *C. trachomatis*. Considering this, we have undertaken the task of outlining the interaction between GrgA and two major σ factors of *C. trachomatis* (σ^{66} and σ^{28}). While we have reported in the past [79] that GrgA contacts the non-conserved region 4 (NCR-4) of σ^{66} and stimulates transcription from many σ^{66}-dependent promoters *in vitro*, we have yet to characterize the GrgA-σ^{28} interaction.

In this chapter, we provide evidence showing that: (i) GrgA can activate transcription from a σ^{28}-dependent promoter *in vitro*; and (ii) σ^{28} and DNA both bind GrgA and share a unique binding site on GrgA, one that is separate from site where σ^{66} binds. Additionally, we use a label-free technology called bio-layer interferometry (BLI) that is routinely employed in the study of protein-protein interactions along with pulldown assays to show that GrgA displays a higher affinity for σ^{66} than from σ^{28} *in vitro*. As a step towards further future research, we also provide initial evidence for the interaction of GrgA with two other parts of the RNA polymerase: the α and β' subunit. Since σ^{28} and σ^{66}, for the most part, control genes involved in two separate temporal stages, the differential regulation of these two σ factors by GrgA indicates that GrgA plays a pivotal role in the temporal regulation of gene expression in the *C. trachomatis* developmental cycle.

RESULTS

GrgA stimulates σ²⁸-dependent transcription from a *hctB* promoter. *In vitro* transcription assays were performed by another member of our laboratory (Dr. Xiaofeng Bao) to ascertain whether or not GrgA activates σ²⁸-dependent transcription. Previous studies have shown that transcription of the promoter sequence of a gene encoding the protein *hctB* in *C. trachomatis* requires the addition of recombinant *C. trachomatis* σ²⁸ to the *C. trachomatis* RNA polymerase [78]. Consistent with these findings, our data indicates that not only is recombinant, purified N-terminally His-tagged σ²⁸ (NH-σ²⁸ in Fig. 4.1A) required for the activation of transcription of a plasmid (pMT1212) that contains the *hctB* promoter sequence (Fig. 4.1B) but that GrgA stimulates this transcription activation in a dose-dependent manner (Fig. 4.1C and 4.1D). Thus, GrgA can stimulate σ²⁸-dependent transcription alongside stimulate σ⁶⁶-dependent transcription.
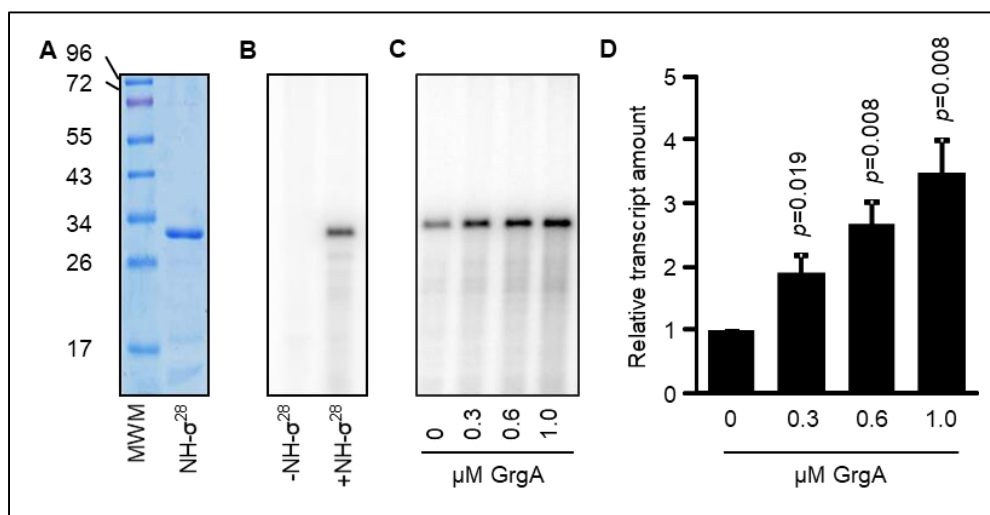
Figure 4.1. GrgA stimulates σ²⁸-dependent transcription using C. trachomatis RNAP. (A) Coomassie Blue stain showing NH-σ²⁸ purified from denatured cell extract and subjected to renaturation. (B) Transcription from the *C. trachomatis* hctB promoter in the pMT1212 report plasmid is dependent on the addition of NH-σ²⁸ to the partially purified chlamydial RNAP. (C) Gel image showing dose-dependent stimulation of transcription from the hctB promoter. (D) Averages and SDs for three independent measurements are shown. All experiments in this figure were performed by Dr. Xiaofeng Bao.

GrgA can pull down σ^{28} *in vitro* and vice versa; the N-terminal lead sequence and region 2 of σ^{28} are required for interaction with GrgA. We performed pulldown assays to determine whether or not GrgA could pulldown σ^{28} *in vitro* and vice versa. Using StrepTactin beads, we successfully co-precipitated: (i) NH-σ^{28} using N-terminally Strep-tagged-GrgA (Fig. 4.2A) and (ii) N-terminally His-tagged GrgA using N-terminally Strep-tagged σ^{28} (Fig. 4.2B). We then constructed (Fig. 4.2C) and purified (Fig 4.2D) four mutants of NH-σ^{28} by deleting either its N-terminal lead sequence or one of its three conserved regions (R2, R3, or R4). We found that, while the deletion of R3 or R4 reduced but did not disable the ability of σ^{28} to pulldown GrgA, the deletion of either the N-terminal lead sequence or R2 completely disabled σ^{28}-pulldown of GrgA (Fig. 4.2E).
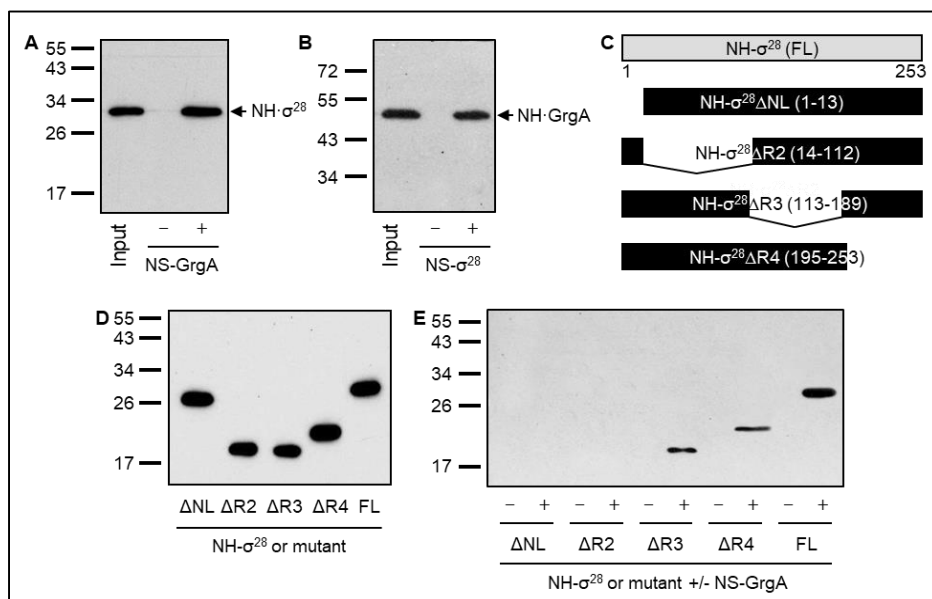
Figure 4.2. The N-terminal lead sequence and region 2 of σ^{28} are required for interaction with GrgA.
(A) Precipitation of NH-σ^{28} by Strep-Tactin-immobilized NS-GrgA. (B) Precipitation of NH-GrgA by Strep-Tactin-immobilized NS-σ^{28}. (C) Schematic of σ^{28} and mutants lacking the indicated regions. (D) Expression of purified NH-σ^{28} and mutants. (E) Precipitation of NH-σ^{28} and mutants by Strep-Tactin-immobilized NS-GrgA. All proteins were resolved via SDS-PAGE and detected using an anti-His antibody. Note that GrgA, as shown previously [79], resolves on a SDS gel much higher (50 kDa) than its theoretical size (33 kDa).

A middle region of GrgA is required to bind σ^{28} *in vitro*. We constructed (Fig. 4.3A) and purified (Fig 4.3B) five mutants of NH-GrgA by deleting roughly 50-60 amino acid residues from the full-length protein to test whether if these residues were required for binding to σ^{28} *in vitro*. Interestingly, NS-σ^{28} was able to co-precipitate all but one construct (Δ114-165) (Fig. 4.3C). Note that, while pulldown assays elsewhere in this project were detected by Western blot using an anti-His antibody, they were detected here by Coomassie-blue stain since at least one of these constructs (Δ1-64) is not recognized by the anti-His antibody. Subsequently, we constructed (Fig. 4.3D) and purified (Fig 4.3E) two constructs with non-overlapping deletions in the 114-165 region in order to test their ability to bind σ^{28} and found that NS-σ^{28} was able to co-precipitate the Δ114-137 but not the Δ138-165 construct (Fig 4.3F).
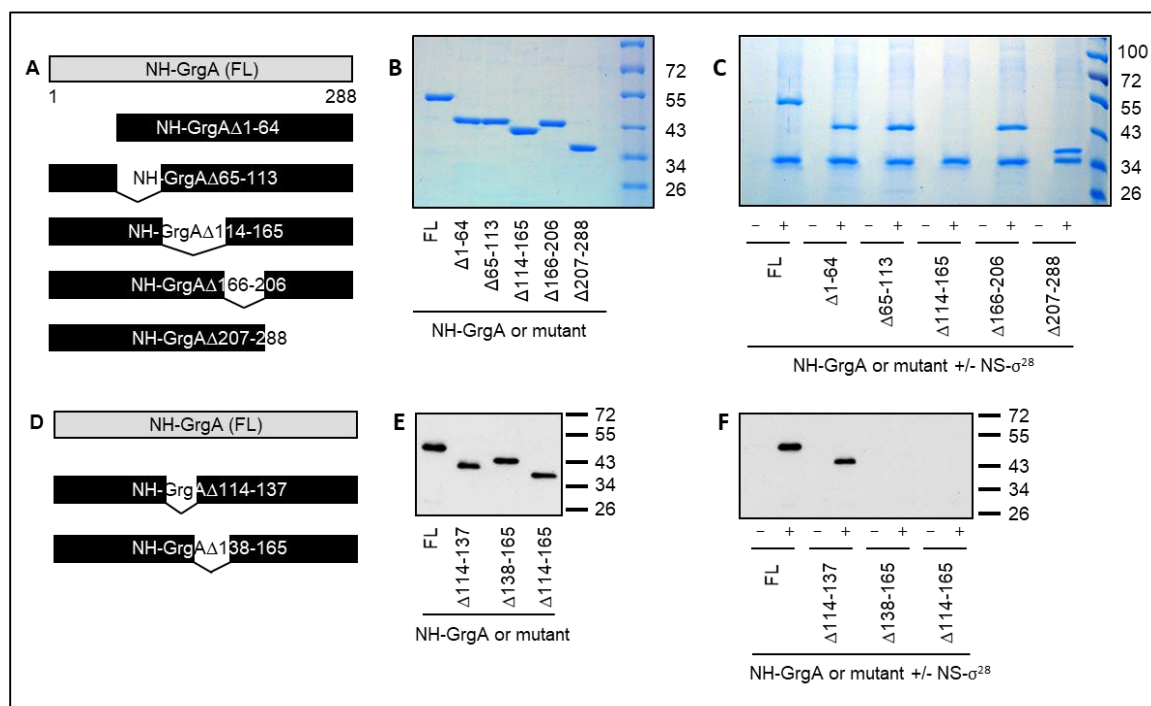
Figure 4.3. A middle region of GrgA is required for binding σ^{28}. (A & D) Schematic of GrgA and mutants with deletions of indicated regions. Expressed proteins were detected by Coomassie-blue stain (B) or western blotting (E). (C) GrgA or deletion mutants pulled down by Strep-Tactin-immobilized NS-σ^{28} were detected by either Commassie-blue stain (B) or western blotting using an anti-His antibody (F).

All residues with the 138-165 region of GrgA are required to bind σ^{28} *in vitro*.

Considering our success with prior experiments, we attempted to further narrow down the residues required for binding to σ^{28} *in vitro*. We constructed (Fig. 4.4A) and purified (Fig 4.4B) four mutants of NH-GrgA with 7 amino acids, non-overlapping deletions in the 138-165 region. However, NS-σ^{28} was able to co-precipitate all four constructs but to reduced ability, indicating that a region bigger than 7 amino acid residues might be required for binding to σ^{28} *in vitro* (Fig. 4.4C). In order to backtrack from this finding, we constructed (Fig. 4.4D) and purified (Fig 4.4E) two mutants of NH-GrgA with overlapping deletions in the 138-165 region. To our surprise, both constructs were pulled down by NS-σ^{28} (Fig 4.4F), indicating that possibly the entire 138-165 region is required for σ^{28}-binding.
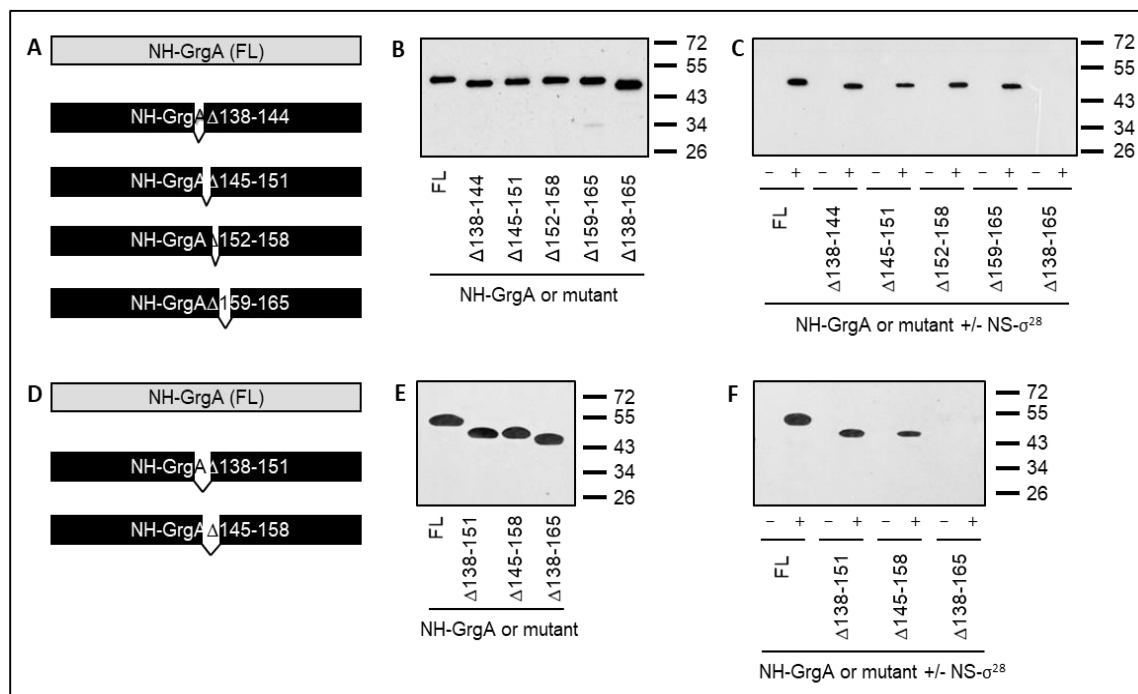
Figure 4.4. All residues with the 138-165 region of GrgA are required to bind σ^{28} *in vitro*. (A & D) Schematic of GrgA and mutants with deletions of indicated regions. Expressed proteins were detected by western blotting (B & E). (C) GrgA or deletion mutants pulled down by Strep-Tactin-immobilized NS-σ^{28} were detected by western blotting using an anti-His antibody (C & F).

The 138-165 region of GrgA is required for binding both σ^{28} and DNA. In our previous study, we showed that GrgA binds DNA in a sequence non-specific manner, and that residues 114-165 of GrgA are required to bind DNA since their deletion inactivates DNA-binding in GrgA [79]. Dr. Xiaofeng Bao used the aforementioned NH-GrgA mutants in electromobility shift assays (EMSA) to test whether if we could isolate a possible sequence shorter than 53 amino acids in GrgA for GrgA to maintain its DNA-binding ability. To our surprise, not only did the Δ138-165 construct fail to bind DNA compared to Δ114-137 (Fig. 4.5A), but any smaller deletion within the 138-165 region did not affect the ability of GrgA to bind DNA (Fig. 4.5B and Fig. 4.5C). Thus, this region binds both σ^{28} and DNA.
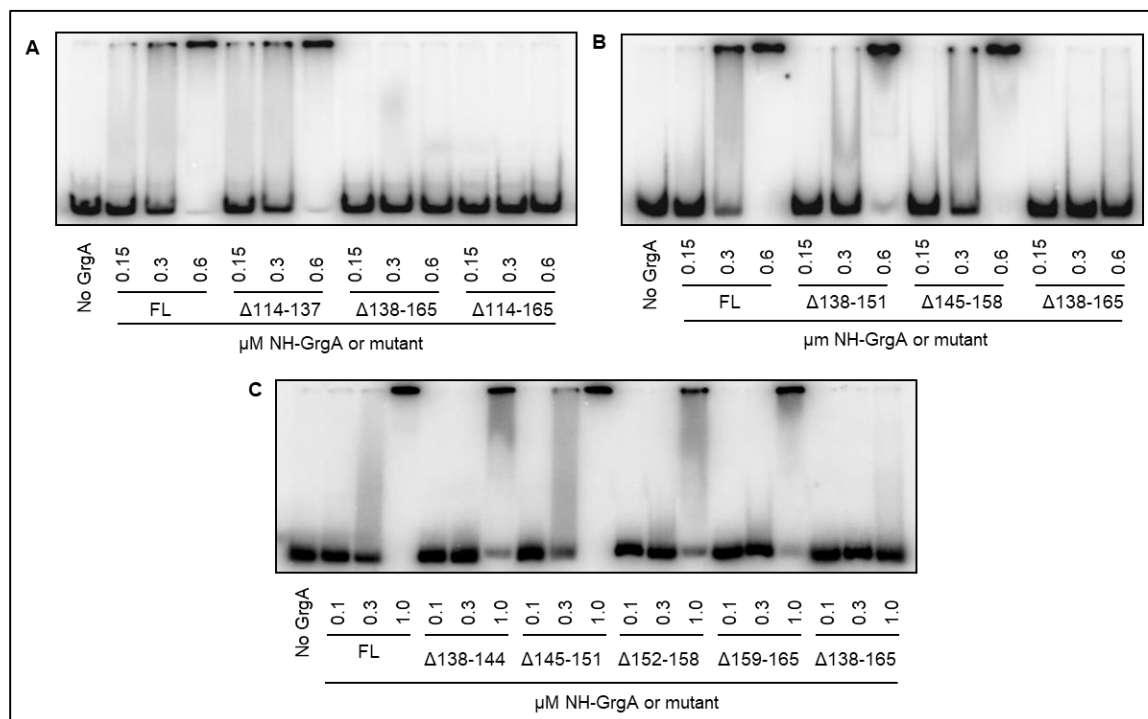
Figure 4.5. Localization of the DNA-binding region in GrgA to residues 138-165. Electrophoresis mobility shift assays were performed using a radiolabeled DNA fragment carrying sequences extending from position –144 to +52 of the *def*A gene in the presence of the indicated concentrations of wild-type GrgA or the indicated GrgA mutant. All experiments in this figure were performed by Dr. Xiaofeng Bao.

The 138-165 region of GrgA is required for σ^{28}-dependent transcription activation. In Fig. 4.1D, we showed that GrgA stimulates σ^{28}-dependent transcription activation in a dose-dependent manner. To test the ability of the aforementioned NH-GrgA mutants to similarly stimulate transcription activation, Dr. Xiaofeng Bao performed *in vitro* transcription assays using these mutants. Consistent with all our pulldown assays, the use of either Δ114-165 or Δ138-165 in transcription assays caused a significant and dramatic 3-fold decrease in transcript levels from those of full-length NH-GrgA (Fig. 4.6). Furthermore, all smaller deletions within the 138-165 region caused a small but not dramatic decrease in transcript levels from full-length NH-GrgA, indicating that multiple or all of these regions may be required for transcription activation (Fig. 4.6). To our surprise, the Δ1-64 construct also experienced a significant 1.5-fold loss in transcription activation compared to full-length GrgA (Fig. 4.6), suggesting that, though Δ1-64 may not be required for GrgA to bind σ^{28} (Fig. 4.3C), the deletion of these residues may affect the structure and function of GrgA and curb its ability to fully stimulate transcription activation.
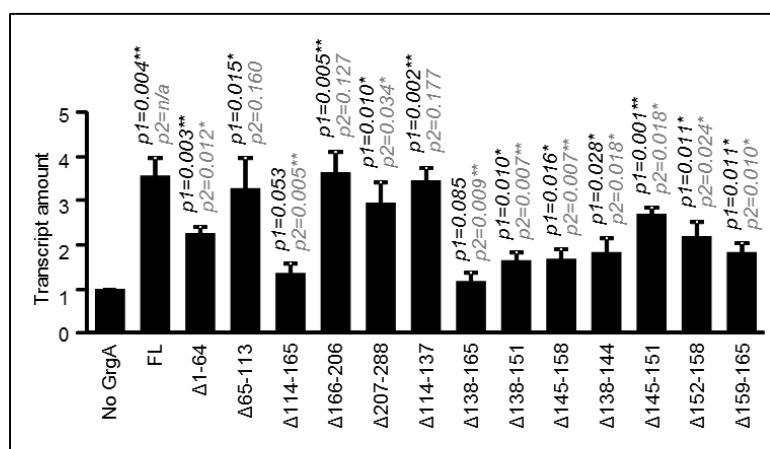
Figure 4.6. Activation of σ^{28}-dependent transcription correlates with σ^{28}-binding in GrgA. Transcription assays were performed using pMT1212 and in the absence or presence of x μM GrgA or the indicated GrgA mutant. *p1* is the p value between basal transcription activity (without GrgA) and activity with GrgA; *p2* is p value between full length GrgA and deletion mutants (paired t tests of 3 or more independent experiments).

GrgA displays a higher affinity for σ⁶⁶ than for σ²⁸ *in vitro*. Since GrgA binds both σ⁶⁶ and σ²⁸ during our experiments, we tested whether GrgA binds both with a similar σ⁶⁶ and NH-σ²⁸, and found that NS-GrgA successfully pulled down both σ factors when encountered individually but not together (Fig. 4.7). Upon encountering both σ factors in a mixture, NS-GrgA could only pull down CH-σ⁶⁶, indicating that GrgA shows a higher affinity for σ⁶⁶ than for σ²⁸ *in vitro,* and that GrgA likely cannot bind both σ factors simultaneously.
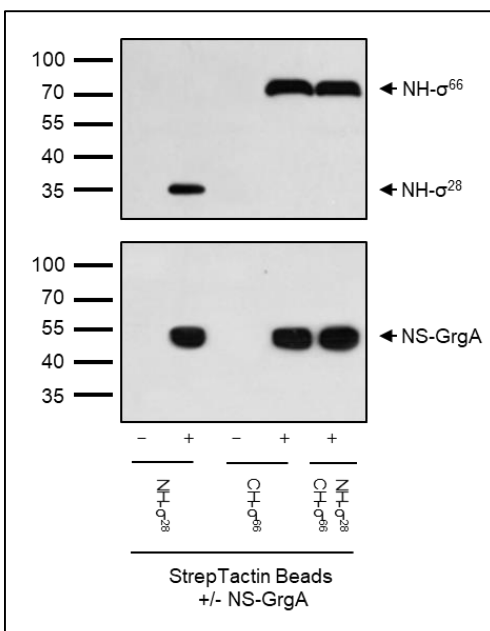
Figure 4.7. GrgA displays higher affinity for σ⁶⁶ than for σ²⁸ *in vitro*. Pull-down of NH-σ²⁸, CH-σ⁶⁶ or both by Strep-Tactin-immobilized NS-GrgA visualized by Western blot with anti-His antibody (above) and anti-Strep antibody (below).

GrgA displays a higher affinity for σ^{66} than for σ^{28} during bio-layer interferometry assays. Since GrgA showed a higher affinity for σ^{66} than for σ^{28} during our pulldown experiments, we used a more sensitive assays, bio-layer interferometry (BLI), to measure the affinity of GrgA to σ^{66} and σ^{28} *in vitro*. BLI detects light wavelength shifts at tip of a biosensor with an immobilized ligand following the binding of an analyte in a real-time manner. When NH-GrgA was used as a ligand, the CS-σ^{66} analyte yielded a statistically significant 25-fold higher k_a than the NS-σ^{28} analyte, suggesting that CS-σ^{66} binds NH-GrgA much faster than NS-σ^{28} (Fig. 4.8A and 4.8B, and Table 4.1). CS-σ^{66} also demonstrated a 3-fold statistically significant increase in k_d, suggestive of moderately higher dissociation from NH-GrgA (Fig. 4.8A and 4.8B, and Table 4.1). Compared to the NH-GrgA-CS-σ^{66} interaction, the NH-GrgA-NS-σ^{28} interaction had a 32-fold higher K_D, indicating that GrgA has a significantly higher overall affinity for σ^{66} than σ^{28} (Fig. 4.8A and 4.8B, and Table 4.1).

Reciprocal BLI using CH-σ^{66} and NH-σ^{28} as ligands and NS-GrgA as the analyte were performed to validate the above difference in GrgA binding by the σ factors. Consistent with the trend in k_a values presented above, the NS-GrgA analyte also demonstrated a statistically significant higher k_a for CH-σ^{66} than for NH-σ^{28} although the difference is smaller (25-fold vs 3.7 fold). Interestingly, the k_d values revealed that NS-GrgA also dissociates from NH-σ^{66} 6-fold slower than from NH-σ^{28} (Fig. 4.8C and 4.8D, and Table 4.1). Compared to the NH-σ^{66}-NS-GrgA interaction, the NH-σ^{28}-NS-GrgA interaction had a 28-fold higher K_D. This difference (28-fold) in K_D values detected in the reciprocal BLI is nearly identical the difference observed with the BLI data presented above (32-fold) (Table 4.1).
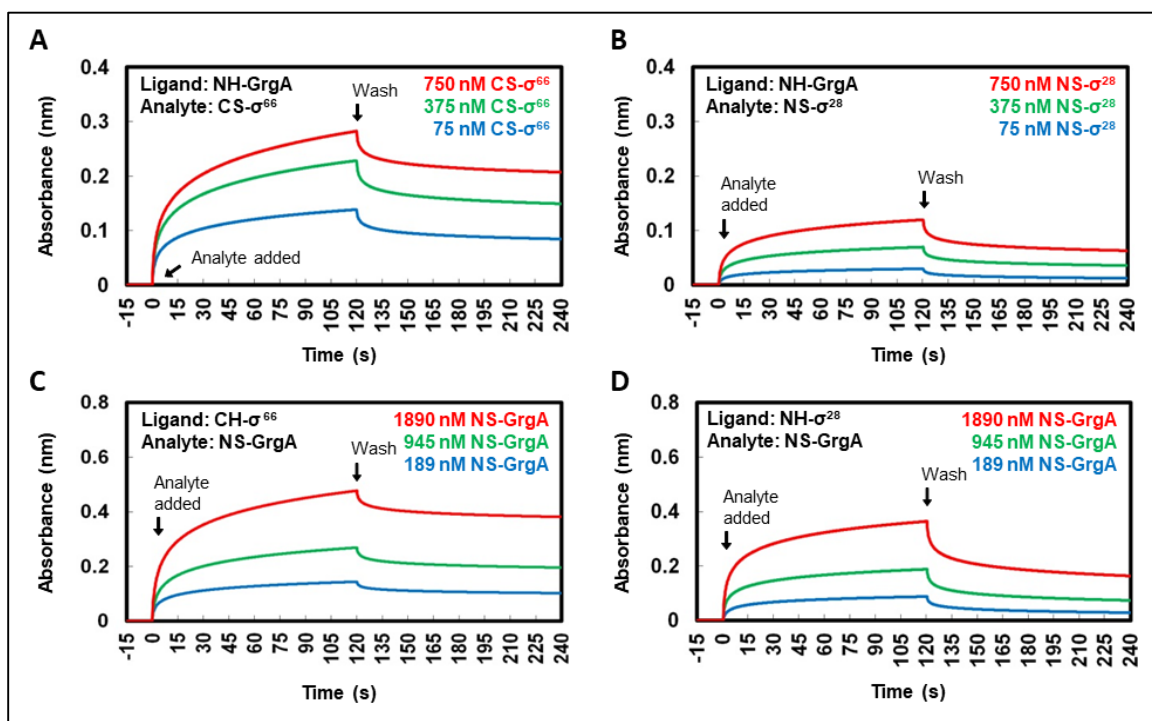
Figure 4.8. GrgA displays higher affinity for σ^{66} than for σ^{28} in vitro. (A-D) BLItz graphs showing real time light absorbance changes upon binding of a Strep-tagged protein (analyte) to an immobilized-His tagged protein (ligand), and subsequent wash.

Table 4.1. GrgA binds σ^{66} with significantly higher affinity than σ^{28}. Shown are the K_D values generated by the BLItz machine upon the association, and subsequent disassociation, of a ligand-analyte pair. K_D, which is inversely related to affinity, is calculated by dividing the disassociation rate constant (k_d) by the association rate constant (k_a). Based on the K_D values, NH-GrgA shows an approximately 32–fold higher affinity for CS-σ^{66} than NS-σ^{28}, and NS-GrgA shows an approximately 28-fold higher affinity for CH-σ^{66} than NH-σ^{28}. n, number of experimental repeats. PC, percent control. p values were calculated using 2-tailed Student's t tests.

Ligand	Analyte	n	k_a		k_d		K_D	
			1/Ms (M ± SD)	PC	1/s	PC	M	PC
NH-GrgA	CS-σ^{66}	6	$(1.9 \pm 1.3) \times 10^6$	100	$(9.3 \pm 5.2) \times 10^{-3}$	100	$(6.9 \pm 5.9) \times 10^{-9}$	100
NH-GrgA	NS-σ^{28}	8	$(1.5 \pm 1.7) \times 10^4$	4.0	$(2.8 \pm 0.8) \times 10^{-3}$	30.0	$(2.2 \pm 1.1) \times 10^{-7}$	3188
			p = 0.001		*p = 0.001*		*p < 0.001*	
CH-σ^{66}	NS-GrgA	4	$(7.7 \pm 1.3) \times 10^5$	100	$(8.9 \pm 0.6) \times 10^{-3}$	100	$(1.2 \pm 0.1) \times 10^{-8}$	100
NH-σ^{28}	NS-GrgA	6	$(2.1 \pm 0.9) \times 10^5$	27.0	$(5.6 \pm 1.2) \times 10^{-2}$	629	$(3.4 \pm 2.0) \times 10^{-7}$	2833
			p < 0.001		*p < 0.001*		*p = 0.013*	

Lack of binding between σ^{66} and GrgA mutant Δ1-64, and σ^{28} and GrgA mutant Δ138-165 during bio-layer interferometry assays. Considering the sensitivity of BLI assays, we used BLI to test whether if GrgA mutants Δ1-64 and Δ138-165 could bind σ^{66} and σ^{28} respectively. Consistent with data published in our previous study [79] and our above pulldown findings (Fig. 4.3F), BLI recorded complete disassociation of CS- σ^{66} from NH-GrgAΔ1-64 after wash (Fig. 4.9A), suggesting a lack of any true binding. Similarly, BLI recorded complete disassociation of NS-σ^{28} from NH-GrgAΔ138-165 after wash (Fig. 4.9B). K_D values for both sets of ligand-analyte interactions could not be calculated due to the complete disassociation of the analyte from the ligand upon wash. These findings suggest that residues 1-64 and 138-165 in GrgA are responsible and required for the binding of σ^{66} and σ^{28} respectively.
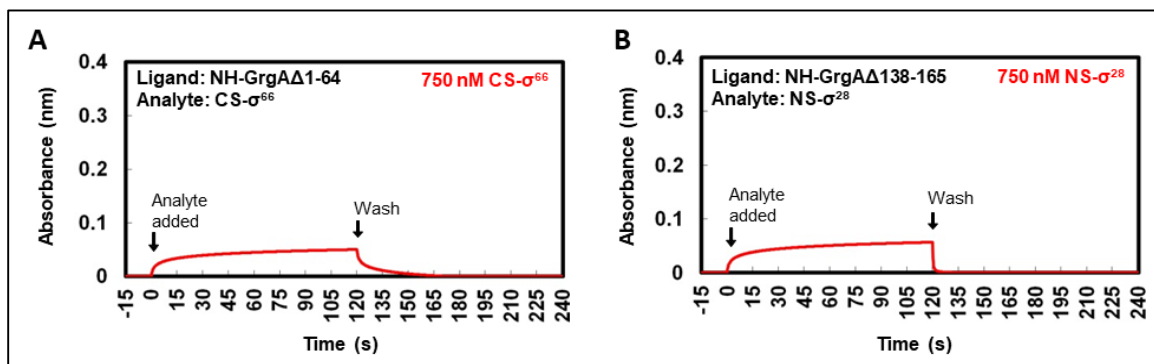
Figure 4.9. Lack of binding between (A) σ^{66} and NH-GrgA Δ1-64 and (B) σ^{28} and NH-GrgA Δ138-165 in vitro. (A-B) BLItz graphs showing real time light absorbance changes upon binding of a Strep-tagged protein (analyte) to an immobilized-His tagged protein (ligand), and subsequent wash.

GrgA mutant Δ1-64, in comparison with full-length GrgA and mutant Δ114-137, shows a decreased affinity to σ^{28} during BLI assays. Considering our findings during *in vitro* transcription assays (Fig. 4.6), we used BLI to test the binding affinity of GrgA mutant Δ1-64 to σ^{28} *in vitro*. Compared to full-length NH-GrgA (Fig. 4.10A and Table 4.2), BLI recorded a moderately slowed association and a moderately accelerated dissociation of NS-σ^{28} from NH-GrgAΔ1-64, as indicated by a nearly 3-fold decrease in the k_a and a 2-fold increase in the k_d CS-σ^{66} from NH-GrgA Δ1-64 after wash (Fig. 4.10B and Table 4.2). These changes resulted in a highly significant 4.8-fold increase in the K_D value. On the other hand, NH-GrgAΔ114-137, which retains the activity to activate σ^{28}-dependent transcription (Fig. 4.6), demonstrated no such changes in parameters in its interaction with NS-σ^{28} (Fig 4.10C and Table 4.2).

GrgA fragment 138-165 can bind σ^{28} in the absence of rest of the protein. Considering that both our pulldown assays (Fig. 4.3F) and aforementioned BLI assays indicated that that 138-165 region of GrgA is required to bind σ^{28} (Fig 4.9), we further tested the ability of a small, 28 amino-acid fragment (138-165) of GrgA to bind σ^{28} through BLI assays. BLI recorded that NH-GrgA fragment 135-165 could bind σ^{28} even with deletions of the amino acid residues 1-134 and 166-288 (Fig. 4.10D), but with a 3.5-fold increase in the overall k_D value compared to full-length NH-GrgA (Table 4.2). Notably, this 3.5-fold increase in the k_D (or decrease in affinity) was largely due to a 2.5-fold decrease in the k_a (Table 4.2), which itself was likely a result of large deletions from both the N- and C-termini of the full-length protein.
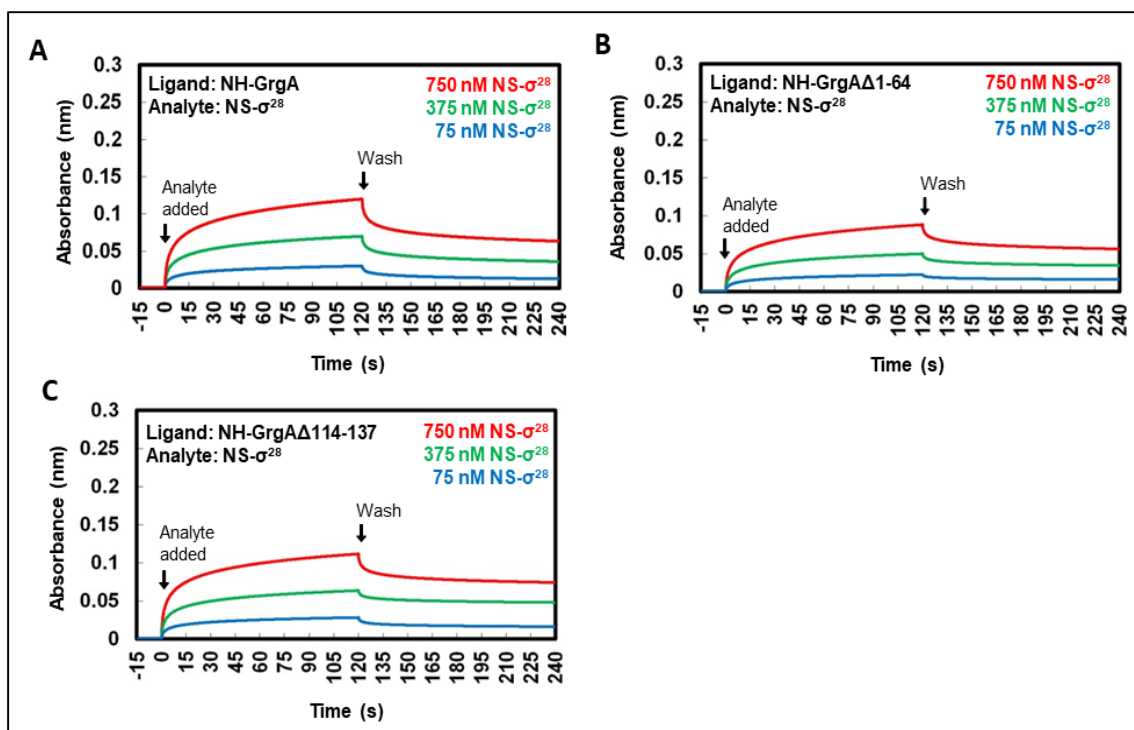
Figure 4.10. GrgA mutant Δ1-64, in comparison with full-length GrgA and mutant Δ114-137, shows a decreased affinity to σ²⁸ during BLI assays. (A-C) BLItz graphs showing real time light absorbance changes upon binding of a Strep-tagged protein (analyte) to an immobilized-His tagged protein (ligand), and subsequent wash.

Table 4.2. A mutant of GrgA defective in transcription activation shows decreased σ²⁸-binding activity. Shown are the K_D values generated by the BLItz machine upon the association, and subsequent disassociation, of a ligand-analyte pair. See Table 1 for information regarding kinetic parameters. n, number of experimental repeats. PC, percent control. p values were calculated using 2-tailed Student's t tests.

Ligand	Analyte	n	k_a		k_d		K_D	
			1/Ms (M ± SD)	PC	1/s	PC	M	PC
NH-GrgA	NS-σ²⁸	8	$(1.5 \pm 1.7) \times 10^4$	100	$(2.8 \pm 0.8) \times 10^{-3}$	100	$(2.2 \pm 1.1) \times 10^{-7}$	100
NH-GrgA-Δ1-64	NS-σ²⁸	4	$(5.6 \pm 2.8) \times 10^3$	37	$(5.8 \pm 2.3) \times 10^{-3}$	200	$(1.1 \pm 0.2) \times 10^{-6}$	479
			p = 0.037		*p = 0.009*		*p < 0.001*	
NH-GrgA-Δ114-137	NS-σ²⁸	4	$(1.5 \pm 0.4) \times 10^4$	98	$(3.5 \pm 0.5) \times 10^{-3}$	124	$(2.5 \pm 0.3) \times 10^{-7}$	112
			p = 0.947		*p = 0.128*		*p = 0.658*	
NH-GrgA-138-165	NS-σ²⁸	3	$(6.0 \pm 1.0) \times 10^3$	40	$(4.6 \pm 0.4) \times 10^{-3}$	164	$(7.7 \pm 0.3) \times 10^{-7}$	350
			p = 0.078		*p = 0.089*		*p = 0.125*	

Deletion of the N-terminal lead sequence or the R2 of σ^{28} results in a severe loss in binding to GrgA. Our pulldown assays (Fig. 4.2E) demonstrated that the N-terminal lead sequence and R2 of σ^{28} are required for binding of GrgA. To substantiate this, we performed BLItz analyses using these His-tagged σ^{28} mutants. However, initial loading of these His-tagged mutants onto the biosensor, unlike in previous assays, was not similar between the mutants, likely due to restricted access to the epitope tag on some proteins. Thus, we decided to use biotinylated-NH-GrgA as a ligand (immobilized on a streptavidin-biosensor instead of a His-biosensor) with His-tagged σ^{28} mutants as analytes. Consistent with our pulldown data, BLItz indicated that the deletion of either the N-terminal lead sequence or the R2 of σ^{28} results in a dramatic decrease (360- or 200-fold respectively) in affinity to biotinylated-NH-GrgA compared to full-length σ^{28} (Fig. 4.11 and Table 4.3). Interestingly, BLItz also showed that the deletion of R3 or R4 from σ^{28} also caused a 7-fold decrease in affinity (Fig. 4.11D and 4.11E, and Table 4.3), which was not demonstrated by our pulldown assay (Fig. 4.2E). The decreases in k_D, in each case, were due to increased disassociation rather than decreased association (Table 4.3).
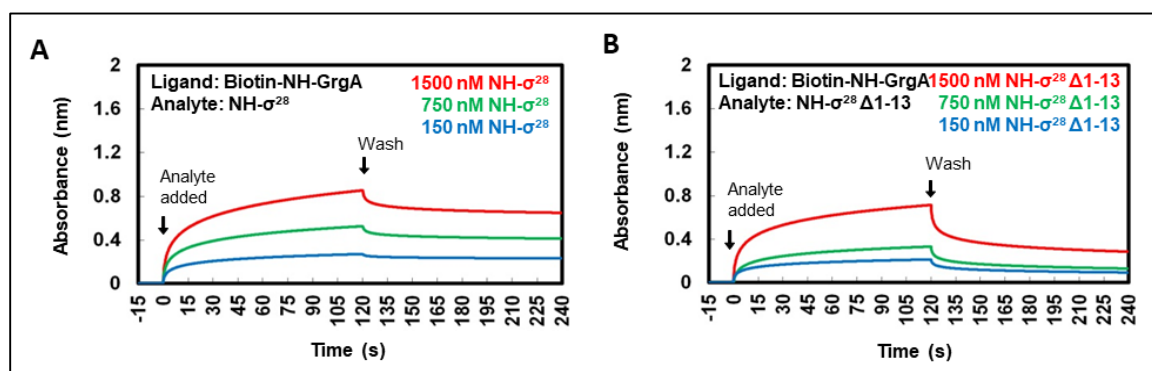
Figure 4.11. Deletion of the N-terminal lead sequence or the R2 of σ^{28} results in a strong decrease in binding to GrgA. (A-E) BLItz graphs showing real time light absorbance changes upon binding of a His-tagged protein (analyte) to an immobilized-biotinylated tagged protein (ligand), and subsequent wash.
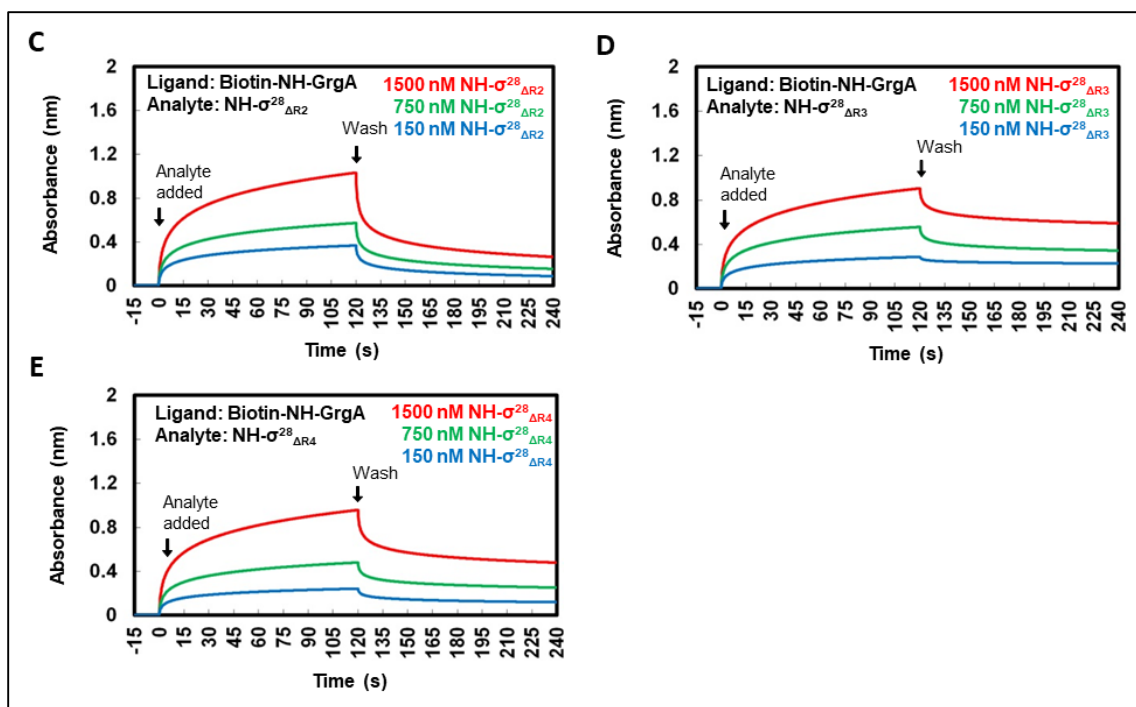
Figure 4.11 (continued). Deletion of the N-terminal lead sequence or the R2 of σ²⁸ results in a strong decrease in binding to GrgA. (A-E) BLItz graphs showing real time light absorbance changes upon binding of a His-tagged protein (analyte) to an immobilized-biotinylated tagged protein (ligand), and subsequent wash.

Table 4.3. Deletion of the N-terminal lead sequence or the R2 of σ²⁸ results in a strong decrease in binding to GrgA. Shown are the K_D values generated by the BLItz machine upon the association, and subsequent disassociation, of a ligand-analyte pair. See Table 1 for information regarding kinetic parameters. n, number of experimental repeats. PC, percent control. Note that 2-tailed Student's t tests were not performed for these sets of data.

Biotinylated Ligand	Analyte	n	k_a		k_d		K_D	
			1/Ms (M ± SD)	PC	1/s	PC	M	PC
NH-GrgA	NH-σ²⁸	3	$(2.2 \pm 0.4) \times 10^4$	100	$(4.7 \pm 0.1) \times 10^{-3}$	100	$(2.1 \pm 0.3) \times 10^{-7}$	100
NH-GrgA	NH-σ²⁸-Δ1-13	3	$(2.4 \pm 0.4) \times 10^4$	109	$(1.8 \pm 0.2) \times 10^0$	38297	$(7.7 \pm 1.0) \times 10^{-5}$	36666
NH-GrgA	NH-σ²⁸_{ΔR2}	3	$(1.3 \pm 0.4) \times 10^4$	59	$(5.3 \pm 0.8) \times 10^{-1}$	11276	$(4.3 \pm 0.6) \times 10^{-5}$	20476
NH-GrgA	NH-σ²⁸_{ΔR3}	3	$(8.0 \pm 1.6) \times 10^4$	363	$(1.2 \pm 0.2) \times 10^{-1}$	2553	$(1.5 \pm 0.3) \times 10^{-6}$	714
NH-GrgA	NH-σ²⁸_{ΔR4}	3	$(3.3 \pm 0.5) \times 10^4$	150	$(4.9 \pm 1.0) \times 10^{-2}$	1043	$(1.5 \pm 0.4) \times 10^{-6}$	714

The non-conserved region of σ⁶⁶ is required and adequate for binding GrgA.

In a previous study, we demonstrated that the non-conserved region 4 (NCR-4) of σ^{66} was required for binding GrgA during pulldown assays [79]. To further substantiate this, we performed BLItz analyses using the fragment NH-σ^{66}-NCR as a ligand and NS-GrgA as an analyte. Interestingly, NH-σ^{66}-NCR was able to bind NS-GrgA (Fig. 4.12B), but with a 5-fold increase in k_D from full-length CH-σ^{66} (Fig. 4.12A and Table 4.4). This decrease in affinity was likely the result of a similar 6-fold decrease in the k_a compared to full-length CH-σ^{66} as the k_d remained largely unaffected between the two proteins (Table 4.4).
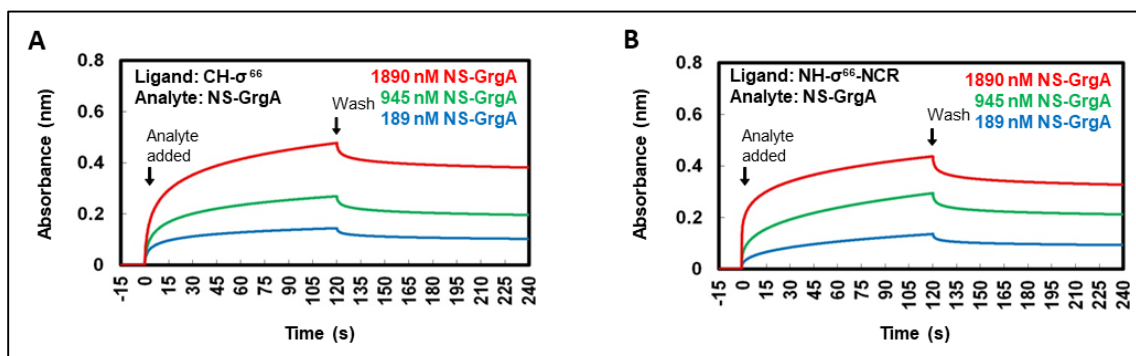
Figure 4.12. The non-conserved region (NCR) of σ⁶⁶ binds to GrgA in isolation with similar affinity as full-length σ⁶⁶. BLItz recordings showing NH-σ^{66}NCR (ligand) binding to NS-GrgA (analyte).

Table 4.4. The non-conserved region of σ⁶⁶ is required and adequate for binding GrgA. Shown are the K_D values generated by the BLItz machine upon the association, and subsequent disassociation, of a ligand-analyte pair. See Table 1 for information regarding kinetic parameters. n, number of experimental repeats. Note that 2-tailed Student's t tests were not performed for these sets of data.

Ligand	Analyte	n	k_a		k_d		K_D	
			1/Ms (M ± SD)	PC	1/s	PC	M	PC
CH-σ^{66}	NS-GrgA	4	$(7.7 \pm 1.3) \times 10^5$	100	$(8.9 \pm 0.6) \times 10^{-3}$	100	$(1.2 \pm 0.1) \times 10^{-8}$	100
NH-σ^{66}-NCR	NS-GrgA	3	$(1.2 \pm 0.3) \times 10^5$	15.5	$(7.8 \pm 1.0) \times 10^{-3}$	87.6	$(6.5 \pm 1.0) \times 10^{-8}$	543

GrgA binds both the α and β' subunit of the chlamydial RNA polymerase.

Considering that GrgA binds two σ factors and has been shown to contact the RNA polymerase holoenzyme for activating transcription, we theorized that GrgA also binds other subunits of the RNA polymerase individually. In order to test this, we performed BLItz analyses using GrgA and the α (RpoA) and β' (RpoC) subunits of the chlamydial RNA polymerase. BLItz demonstrated that NS-GrgA binds both NH-RpoA and NH-RpoC (graphs not shown), but that it binds β' with a slightly higher affinity than the α subunit (Table 4.5).

Table 4.5. The α and β' subunit of the chlamydial RNA polymerase can bind GrgA *in vitro*. Shown are the K_D values generated by the BLItz machine upon the association, and subsequent disassociation, of a ligand-analyte pair. See Table 1 for information regarding kinetic parameters. n, number of experimental repeats. PC, percent control. Note that 2-tailed Student's t tests were not performed for these sets of data.

Ligand	Analyte	n	k_a	k_d	K_D
			1/Ms (M ± SD)	1/s	M
NH-RpoA	NS-GrgA	3	$(2.2 \pm 0.4) \times 10^4$	$(1.3 \pm 0.2) \times 10^{-3}$	$(5.7 \pm 1.2) \times 10^{-7}$
NH-RpoC	NS-GrgA	3	$(9.6 \pm 1.2) \times 10^4$	$(1.4 \pm 0.4) \times 10^{-3}$	$(1.5 \pm 0.3) \times 10^{-8}$
CH-σ^{66}	NS-GrgA	4	$(7.7 \pm 1.3) \times 10^5$	$(8.9 \pm 0.6) \times 10^{-3}$	$(1.2 \pm 0.1) \times 10^{-8}$
NH-σ^{28}	NS-GrgA	6	$(2.1 \pm 0.9) \times 10^5$	$(5.6 \pm 1.2) \times 10^{-2}$	$(3.4 \pm 2.0) \times 10^{-7}$

DISCUSSION

A unique, biphasic developmental cycle remains the single most unifying feature tying together members of the genus *Chlamydia*. Highly conserved amongst the various species of *Chlamydia* regardless of the range of host species that they infect, the developmental cycle of *Chlamydia* is marked by a level of sophistication and complexity that is usually reserved for higher eukaryotes rather than prokaryotes and, as such, has proved a very compelling topic for bacterial research. The events of the chlamydial developmental cycle are often summarized into 5 broad phases, including attachment and entry of the elementary body (EB) into the host, differentiation of the EB to the reticulate body (RB), proliferation of the RB, secondary differentiation of the RB to the EB, and EB release from host. Considering that the completion of one entire cycle takes only between 48-72 hours, researchers theorize that gene and protein expression inside *C. trachomatis* is very tightly regulated during each of the 5 phases in order to allow smooth transition between the two cellular forms (EB and RB).

While regulation at the translational and post-translational level is possible and has been reported in *C. trachomatis* [80-82], regulation of genes at the transcriptional level, possibly through transcriptional factors, is likely the most important point of control in the developmental cycle of *C. trachomatis*. Microarray and RNA-sequencing studies performed in recent years have validated this notion, including the possibility of temporal gene expression inside *C. trachomatis* [62-66]. Nonetheless, the specific pathways for how genes are temporally regulated in *C. trachomatis* have yet to be uncovered, although studies detailing the actions of transcription factors inside *C. trachomatis* have been recorded by both other researchers [83-85] and members of our own laboratory in the past [79]. In order

to fully understand the scope of transcriptional regulation in *C. trachomatis*, it is crucial to analyze the interaction between transcription factors that exert stimulatory or inhibitory control over the expression of genes such as the one discovered by our laboratory, GrgA, and the chlamydial RNA polymerase, which carries out the transcription.

In this chapter, I have characterized the interaction of GrgA with various parts of the RNA polymerase holoenzyme. Through a mix of pulldown experiments, *in vitro* transcription assays, and protein-protein interaction studies using bio-layer interferometry (BLI), I have extensively detailed the relationship between GrgA and the two major σ factors found in *C. trachomatis* (σ^{28} and σ^{66}). Our findings can be abridged into five, previously undisclosed conclusions: (i) GrgA binds σ^{28} and stimulates transcription activation of σ^{28}-dependent genes; (ii) all regions, but especially the N-terminal lead sequence and the R2, of σ^{28} contribute to binding with GrgA; (iii) a middle region of GrgA, approximately 28 amino acids in length, is required to bind both σ^{28} and DNA; (iv) GrgA shows higher affinity for σ^{66} than for σ^{28} *in vitro*; and (v) GrgA binds the α and β' subunit of the chlamydial RNA polymerase *in vitro*.

The leading discovery in this report is that GrgA binds σ^{28} and stimulates transcription activation of σ^{28}-dependent genes, which we have demonstrated using a pulldown assay (Fig. 4.2A and 4.2B) and an *in vitro* transcription assay (Fig. 4.1C and 4.1D) respectively. Considering that GrgA also stimulates transcription activation of σ^{66}-dependent genes [79] and that σ^{28} and σ^{66} mainly control genes in two separate stages of the chlamydial developmental cycle [73, 74, 76-78], this finding suggests that GrgA is involved in regulation at many different phases of the cycle.

Next, I have made extensive efforts to detail and map the binding regions on GrgA and σ^{28} for each other. My pulldown experiments using deletion mutants of σ^{28} (Fig. 4.2C) indicate that deletion of either the lead sequence or R2 of σ^{28} leads to a complete inactivation of binding to GrgA (Fig. 4.2E). This finding is supported by my corresponding BLItz findings that show 360- and 200-fold drops in affinity to GrgA from full-length of σ^{28} upon deletion of the N-terminal lead sequence and R2 respectively (Table 4.3). Interestingly, my BLItz findings indicate that the deletion of R3 and R4 also affects binding of σ^{28} to GrgA to some extent (Table 4.3), which is also demonstrated, with lesser clarity, by my pulldown experiment (Fig. 4.2E). Together, these data indicate that all regions of σ^{28} contribute to some extent to the binding of σ^{28} to GrgA. By comparison, the non-conserved region (NCR) of σ^{66} alone is sufficient and adequate for binding GrgA (Fig. 4.12 and Table 4.4).

To map the region of GrgA that is responsible for binding σ^{28}, we constructed five initial GrgA mutants with 50 to 80 amino acid deletions (Fig. 4.3A), and eight subsequent GrgA mutants with more localized deletions (Fig. 4.3A, 4.4A, and 4.4D). My pulldown experiments with these mutants show that the deletion of a middle region of GrgA, specifically amino acid residues 138-165, renders it unable to bind σ^{28} (Fig. 4.3C and 4.3F) and that any further deletion within this region (either overlapping or non-overlapping with other deletions) restores binding to some extent (Fig. 4.4C and 4.4F), indicating that all 28 amino acids may be required for σ^{28}-binding. Once again, this notion is supported by our corresponding findings in (a) BLItz that show that deletion of the 138-165 amino acid region in GrgA completely inactivates σ^{28}-binding (Fig. 4.9B) and (b) *in vitro* transcription assays that show a significant 3-fold decrease in transcript levels with the use of

GrgAΔ138-165 compared to full-length GrgA (Fig. 4.6). Furthermore, BLItz showed that a small GrgA fragment, 138-165, with deletions in both its N- and C-termini, can sufficiently bind σ^{28} on its own (Fig. 4.10D and Table 4.3).

To our surprise, our transcription assay involving a σ^{28}–dependent promoter also showed a 1.5-fold reduction in transcript levels from those of full-length GrgA with the use of GrgAΔ1-64 (Fig. 4.6). Since a lack of binding between this construct and σ^{28} was not demonstrated by our pulldown experiments (Fig. 4.3C), I put this finding to test by performing BLItz analysis using this mutant. BLItz confirmed that the deletion of amino acid residues 1-64 somehow reduces the affinity of GrgA to σ^{28} (Table 4.2), even though this region itself may not be directly involved in binding (Table 4.3C). Interestingly, in a previous study, we showed using a pulldown experiment that the deletion of these residues renders GrgA incapable of binding σ^{66} [79], a finding that we have validated here using BLItz experiments (Fig. 4.9A). Considering that this region seems to alter transcription activation for both σ factors, we theorize that these residues, while not directly involved in σ^{28}-binding, may be important in helping GrgA carry out its general functions and that their deletion may severely alter the rest of the protein structure.

Interestingly, our attempts at mapping the DNA-binding site on GrgA (Fig. 4.5) show that the same region that is responsible for σ^{28} binding is also responsible for DNA binding. Thus, σ^{28} and DNA share a binding site on GrgA. Whether or not this influences the binding of either σ^{28} or DNA inside *C. trachomatis* and whether if GrgA can bind both concurrently remains to be detailed, but preliminary competition assays performed using σ^{28} and DNA in combination with GrgA suggests that GrgA might be able to bind DNA in the presence of σ^{28} (data not shown).

Since GrgA binds both σ^{28} and σ^{66}, it is important to explore whether if GrgA shows a preference for binding one σ factor over the other. My extensive BLItz experiments (Table 4.1) indicate that GrgA shows an average 30-fold higher affinity for σ^{66} than for σ^{28} *in vitro*, and my corresponding pulldown experiment (Fig. 4.7) indicates that GrgA may not bind σ^{28} and σ^{66} concurrently. Since σ^{66}, as the primary housekeeping σ factor in *C. trachomatis,* exerts control over many important genes such as MOMP [75], this preference for σ^{66} over σ^{28} is not entirely surprising.

As a step toward future research, I have attempted to characterize the interaction of GrgA with the subunits of the chlamydial RNA polymerase core enzyme, namely the α, β, and β' subunits. While I was able to purify and characterize the interaction of GrgA with the α and β' subunit, I was unable to purify the β as it enters inclusion bodies inside many *E. coli* expression cell lines. Nonetheless, my preliminary findings indicate that GrgA binds both the α and β' subunit of the RNA polymerase (Table 4.5), and does so at nM ranges. We are currently working towards developing a method for co-expressing recombinant chlamydial RNA polymerase (including all three subunits) with GrgA and σ^{66} in order to test whether GrgA can help these proteins fold properly and rescue them being trapped in inclusion bodies. Regardless, we consider it critical that a study investigating the interaction between (a) GrgA and the individual RNA polymerase subunits and (b) GrgA and the RNA polymerase holoenzyme is performed in the future.

In summary, our findings in this report indicate that GrgA is (i) a highly specific transcription factor not found in other bacterial species; (ii) capable of exerting influence over multiple stages of the chlamydial development cycle over as seen by its ability to regulate transcription of both σ^{28}- and σ^{66}-dependent genes; and (iii) able to bind a large

portion of the chlamydial transcriptional machinery, including σ^{28}, σ^{66}, DNA, and two of the RNA polymerase subunits. As such, these findings have significant implications for the research world considering that they outline GrgA as a very strong candidate for the target of novel therapeutic drugs against *C. trachomatis*.

MATERIALS AND METHODS

Reagents. All DNA primers were custom-synthesized at Sigma Aldrich. The QuikChange Site-Directed Mutagenesis Kit, BL21(DE3) ArcticExpress *E. coli* competent cells were purchased from Agilent Technologies. Taq Polymerase, Q5 Site-Directed Mutagenesis Kit, and deoxynucleotides were purchased from New England BioLabs. Isopropyl β-D-1-thiogalactopyranoside (IPTG) was purchased from Gold Biotechnologies. TALON Metal Affinity Resin was purchased from Takara. The StrepTactin Superflow High Capacity Resin and D-desthiobiotin were purchased from IBA Life Sciences. Coomassie Brilliant Blue G-250 Dye, mouse monoclonal anti-Histidine antibody (H1029), and goat anti-mouse horseradish-perodixase-conjugated antibody (A4416), and EZ-Link Sulfo-NHS-LC-Biotin were purchased from Sigma Aldrich. SuperSignal West Pico PLUS Chemiluminescent Substrate was purchased from ThermoFisher Scientific. Dip and Read Ni-NTA (NTA) biosensors were purchased from Pall ForteBio. The HNE Buffer contained 50 mM HEPES (pH 7.4), 300 mM NaCl, and 1 mM EDTA. The HNEG Buffer contained 50 mM HEPES (pH 7.4), 300 mM NaCl, 1 mM EDTA, and 7M Guanidine HCl. The TNE Buffer contained 25 mM Tris (pH 8.0), 150 mM NaCl, and 1 mM EDTA. The TNAM Buffer contained 25 mM Tris-HCl (pH 8.0), 150 mM NaCl, 375 mM Arginine, and 500 mM Mannitol. The Protein Storage (PS) Buffer contained 25 mM Tris-HCl (pH 8.0), 150 mM NaCl, 0.1 mM EDTA, 10 mM $MgCl_2$, 0.1 mM DTT, and 30% glycerol (w/v). The BLItz Buffer contained 25 mM Tris-HCl (pH 8.0), 150 mM NaCl, 0.1 mM EDTA, 10 mM $MgCl_2$, and 0.1 mM DTT.

Vectors. Plasmids for expressing His- or Strep-tagged GrgA, σ^{66}, σ^{28}, and their mutants are listed near the end of this section. Primers used for constructing expression

plasmids (GrgA deletion mutants, NS-σ^{28}) and a DNA fragment for EMSA assays are listed near the end of this section.

Expression of recombinant proteins and preparation of cell extract for purification. BL21(DE3) ArcticExpress *E. coli* cells transformed with a plasmid for expressing an epitope-tagged chlamydial protein (GrgA, σ^{28}, σ^{66} or their mutant) (Table S1) were cultured in the presence of 1 mM IPTG overnight at 15 $^\circ$C in a shaker. Cells were collected by centrifugation, resuspended in one of the following buffers: HNE buffer (for purification of native His-tagged proteins), HNEG buffer (for purification of denatured His-tagged proteins), or TNE buffer (for purification of native Strep-tagged proteins). The cells were disrupted using a French Press. The cell extract was subjected to high-speed (20,000g) centrifugation at 4 $^\circ$C for 30 minutes. Supernatant was collected and used for protein purification.

Purification of Strep-tagged proteins. Strep-tagged GrgA and σ factors were purified as previously described [86]. The supernatant of centrifuged cell lysate was incubated with the StrepTactin superflow high capacity resin on a nutator for 1 h at 4 $^\circ$C. The resin was packed onto a column and washed with 30 column volumes of the TNE Buffer, and then eluted with the TNE Buffer containing 2.5 mM D-desthiobiotin. The elution was collected in 10 fractions. Protein in the fractions was examined following SDS-PAGE and Coomassie-Blue staining. Fractions with high purity and concentration were pooled and dialyzed overnight against the PS Buffer at 4 $^\circ$C, and then stored in aliquots at -80 $^\circ$C.

Purification of His-tagged proteins. The supernatant of centrifuged cell lysate was incubated with the TALON metal affinity resin on a Nutator for 1 hour at 4 °C. The resin incubated with non-denatured cell extract was packed onto a column, washed with 30 column volumes of HNE Buffer containing 1% NP-40, and eluted with the HNE Buffer containing 250 mM imidazole. The resin incubated with denature cell extract was packed onto a column, washed with 30 column volumes of HNEG Buffer, and eluted with HNEG Buffer containing 250 mM Imidazole. Examination of protein purity, dialysis and storage were carried out in the same manner as for purified Strep-tagged proteins [86].

In vitro transcription assay. *In vitro* transcription of σ^{28}-dependent promoter was performed as previously described [79]. The assay in a total volume of 30 µl contained 200 ng supercoiled plasmid DNA, 50 mM potassium acetate, 8.1mM magnesium acetate, 50 mM Tris acetate (pH8.0), 27 mM ammonium acetate, 1 mM DTT, 3.5% (wt/vol) poly-ethylene glycol (average molecular weight, 8,000), 330 µM ATP, 330 µM UTP,1 µM CTP,0.2 µM [α-^{32}P]CTP (3,000 Ci/mmol), 100 µM 3'-O-methyl-GTP, 20 units of RNasin, RNAP, and indicated amount of GrgA or GrgA mutant. The reactions using cRNAP and σ^{28} contained 1.0 µL purified cRNAP and 30nM His-tagged σ^{28}, purified by procedures involving denaturing and refolding as described above. For reactions using eCore and σ^{28}, their concentrations were 5 nM and 30 nM, respectively. The reaction was allowed to pursue at 37 °C for 40 min and terminated by the addition of 70 µL of 2.86 M ammonium acetate containing 4mg of glycogen. After ethanol precipitation, 32P-labeled RNA was resolved by 8M urea–6% polyacrylamide gel electrophoresis, and quantified with a Storm Phosphorimager and the ImageQuant software. Relative amounts of transcripts were presented with that of the control reaction set as 1 unit. Data shown in bar graphs represent

averages ± SDs from three or more independent experiments. Pairwise, two-tailed Student

t tests were used to compare data.

Electrophoresis mobility shift assay (EMSA). GrgA-DNA interaction was determined by EMSA as described previously [79]. ^{32}P-labeled DNA fragment containing the PDF promoter was amplified using a 32P-labeled 5' primer and an unlabeled 3' primer and purified with a Qiagen column. The GrgA-DNA binding reaction was performed in a total volume of 10 μL, containing 10 nM promoter fragment, an indicated amount of NH-GrgA, 1 mM potassium acetate, 8.1 mM magnesium acetate, 50 mM Tris acetate (pH 8.0), 27 mM ammonium acetate, 1 mM DTT, and 3.5% (wt/vol) polyethylene glycol (average molecular weight, 8,000). After mixing for 1 h at 4 °C, the binding mixture was resolved by 6% non-denaturing polyacrylamide gel. Free and GrgA-bound DNA fragments were visualized on a Storm Phosphorimager (Molecular Dynamics).

Pull-down assays. 20 μl of StrepTactin superflow high-capacity resin was washed twice with the HNE Buffer and incubated with 50 μl of Strep-tagged cell extract or purified protein on a Nutator at 4°C for 1 h. The resin was washed three times with HNE Buffer containing 1% NP-40, and then incubated with 5 μg of a purified His-tagged protein (or mutant) on a Nutator at 4 °C for 1 h. After 3 washes with the HNE Buffer containing 1% NP-40 and a final wash with PBS, the resin was eluted using SDS-PAGE sample buffer. All protein was resolved via SDS-PAGE and detected by either Coomassie blue staining or western blotting using a monoclonal mouse anti-His primary antibody and HRP-conjugated goat anti-mouse secondary antibody.

Bio-layer interferometry assay. An NTA biosensor was subjected to initial hydration in BLItz Buffer for 10 minutes before being loaded onto the ForteBio BLItz machine and washed with BLItz Buffer for 30 seconds to obtain a baseline reading. The biosensor was then incubated with 4 µl of a His-tagged ligand for 240 seconds. After a brief wash with BLItz Buffer for 30 seconds to remove excess protein, the biosensor was incubated with 4 µl of an analyte (purified Strep-tagged protein) for 120 seconds to measure association of the ligand-analyte complex. Subsequently, the biosensor was washed with BLItz Buffer for 120 seconds to measure disassociation of the ligand-analyte complex. All BLItz recordings were subsequently fit to a 1:1 binding model using the BLItz Pro software (version 1.1.0.31), which generated the association rate constant (k_a), disassociation rate constant (k_d), and disassociation equilibrium constant (K_D) for each interaction.

CHAPTER V

Identification of GrgA-Associated Proteins in *Chlamydia trachomatis* Using Mass Spectrometry

ABSTRACT

The intracellular bacterium *Chlamydia trachomatis* is characterized by a unique and biphasic developmental cycle that is thought to be transcriptionally controlled. While the promoters of a number of chlamydial genes have been shown to be temporally regulated, only a few transcription factors possessing the ability to regulate transcription in *C. trachomatis* have been outlined in any detail. GrgA is a *Chlamydia*-specific protein that was first identified in 2011 by us as a transcriptional activator of σ^{66}-dependent promoters. In the years since, we have shown that GrgA directs transcription from σ^{28}-dependent promoters in addition to σ^{66}-dependent promoters, and that it shows a differential affinity for these two σ factors of *C. trachomatis*. Considering that GrgA has the ability to contact both σ factors and that some of our unpublished work indicates that it interacts with subunits of the chlamydial RNA polymerase itself, we reason that GrgA may also associate with other proteins to direct processes inside *C. trachomatis*. In this study, we perform mass spectrometry to isolate any possible proteins that associate with GrgA. Using an inducible gene expression system, we overexpress N-terminally His-tagged GrgA inside *C. trachomatis* and test for proteins that are co-enriched with GrgA upon immunoprecipitation with an anti-polyHistidine antibody. Our results suggest that GrgA may contact the RNA polymerase, likely both as a holoenzyme and as individual subunits, and also provide some clues to indicate that GrgA may have roles outside of transcription in *Chlamydia*.

INTRODUCTION

Though research on *Chlamydia* started with the isolation of *C. trachomatis* nearly 60 years ago, all significant steps toward characterizing the transcriptome and proteome of *C. trachomatis* have only been taken near or after the end of the 20th century [87, 88], which is considerably later than for other human pathogens. In fact, prior to 2010, researching involving *C. trachomatis* predominantly focused on genomic or transcriptomic analysis, and protein studies were only performed for a group of localized proteins known to interact with each other. With the arrival of chlamydial transformation and an inducible gene expression system around 2013 [89], the field of chlamydial research has seen a surge in comprehensive genomic, transcriptomic, and even proteomic studies. Quantitative proteomics analysis was actually used to identify many proteins present in the outer membrane complex of *C. trachomatis* [15]. More recently, it has been used by members of the Raphael Valdivia laboratory and the Ian Clarke laboratory to study energy usage inside *C. trachomatis* [28, 29]. Considering that these methods are now employable by most researchers, it is imperative that further proteomic studies involving *C. trachomatis* be performed in order to understand *Chlamydia* from all angles and not just a genomic standpoint as has been the routine for the last 20 years.

In the following pages, we describe our own brief foray into the world of proteomics involving *C. trachomatis*. We use mass spectrometry (MS) to further characterize the actions of a Chlamydia-specific transcription factor, GrgA, that we ourselves identified a few years ago. Through our findings in the previous chapter, we have already established GrgA as a crucial protein involved with both of the chlamydial σ factors, and have provided initial evidence to support the notion GrgA can bind multiple

subunits of the RNA polymerase too. With all this in mind, we use an inducible gene expression system to overexpress N-terminally His-tagged GrgA inside *C. trachomatis* and conduct several immunoprecipitation experiments with two GrgA-directed antibodies, specifically the rabbit anti-GrgA antibody developed by a collaborator ("anti-GrgA #28") and the commonly used anti-polyHistidine antibody. In order to preserve protein-protein interactions in *C. trachomatis* even after cell lysis, we use a combination of two chemical crosslinkers (DSP and DTME) that can readily enter chlamydial cells and fix all interactions.

Even with the advent of quantitative MS, there have been very few studies involving specific proteins in *C. trachomatis* using MS as a detection method, and fewer still geared towards investigating any chlamydial transcriptional factors in general. As such, our study provides plenty of insight and instruction for researchers wishing to identify novel protein-protein interactions through MS both in *Chlamydia* and in other intracellular bacteria. Our study also provides considerable proof to substantiate the notion that GrgA likely spends a significant amount of time in direct contact with the chlamydial RNA polymerase.

RESULTS

Two antibodies (anti-GrgA #28 and mouse anti-polyHistidine) efficiently pull-down GrgA. Since the rabbit anti-GrgA antibody (#28) binds to GrgA itself, it is likely that interaction between this antibody and GrgA may prevent association of other proteins that share the same binding site on GrgA. Therefore, we decided to use an anti-His antibody to immunoprecipitate overexpressed N-terminally His-tagged GrgA (NH-GrgA) in *C. trachomatis*. To do this, we transformed *C. trachomatis* with a Tet-inducible plasmid containing NH-GrgA, infected host cells with these transformed bacteria, added anhydrotetracycline (ahTc) to the samples at three concentrations (0, 1, and 3 nM) at 24 h post-infection to induce protein overexpression from the plasmid, and finally attempted immunoprecipitation of these transformed samples using an anti-His antibody. In order to control for nonspecific binding associated with the presence of the His-GrgA plasmid, we transformed *C. trachomatis* with a control vector (containing green-fluorescent protein in place of His-GrgA) and performed immunoprecipitation of these control vector-transformed *C. trachomatis* samples using the aforementioned anti-His and the anti-GrgA (#28) along with a third nonspecific antibody (rabbit IgG). Induction for these samples was carried out using 3 nM of ahTc. As an additional measure for all samples, a mutant strain of *C. trachomatis* lacking the ability to produce the chlamydial protease-like activity factor, CPAF, was used since CPAF is known to target and breakdown GrgA upon cell lysis. Our data (Fig. 5.1) indicated that, upon induction, GrgA was successfully overexpressed from the plasmid, and successfully pulled down by both of the GrgA-directed antibodies, specifically in endogenous form by the anti-GrgA #28 antibody and in the His-tagged form by the anti-His antibody.
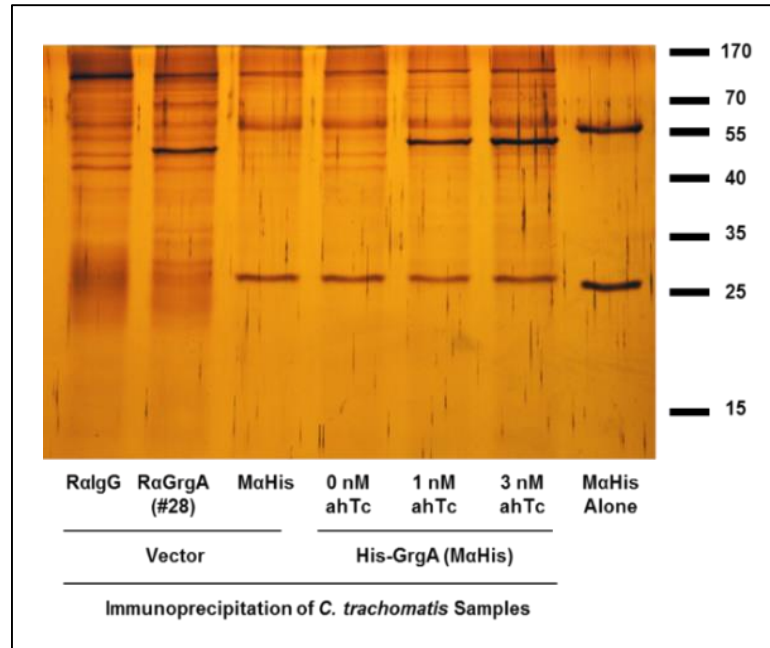
Figure 5.1. Two antibodies (anti-GrgA #28 and anti-His) can pull-down GrgA. Shown is a silver-stain of *C. trachomatis* immunoprecipitation results using three antibodies, including two GrgA-directed antibodies (rabbit anti-GrgA #28 and mouse anti-His) and one control antibody (rabbit IgG). Also shown are heavy and light chains of the anti-His. Bands for GrgA are seen at 50 kDa.

The anti-His antibody is more efficient at pulling down GrgA than the anti-GrgA antibody #28. We next performed a similar immunoprecipitation experiment as the one above, but with a few changes. Instead of silver staining, we used mass spectrometry (MS) as a detection method. While the list of proteins in the immunoprecipitated samples was roughly the same between the two GrgA-directed antibodies and nonspecific peptide counts were low in control antibodies, the peptide counts, for nearly all proteins precipitated, were much higher with the anti-His antibody than with the anti-GrgA #28. Notably, immunoprecipitation using control antibodies or using the anti-His antibody with a control vector did not result in any significant pulldown. Table 5.1 provides a list of 20 genes whose protein products were the most abundant for immunoprecipitation samples prepared with either the anti-GrgA #28 or the anti-His antibody along with the peptide counts recorded by MS for each protein.

Table 5.1. Pulldown of GrgA is more efficient with the anti-His than with the anti-GrgA #28. Shown are the 20 most abundant proteins (along with their peptide counts) reported by MS for *C. trachomatis* samples that were (i) transformed with His-GrgA-containing plasmid, induced, and immunoprecipitated using anti-His antibody or (ii) transformed with control vector, induced, and immunoprecipitated using anti-GrgA #28. GrgA and subunits of the RNA polymerase are denoted in green.

anti-His		anti-GrgA #28	
Gene	Count	Gene	Count
NH-grgA	111	cafE	38
cafE	16	grgA	24
tufA	15	ylqc	12
tsf	14	tufA	10
ompA	14	tsf	10
dnaK	13	recA	9
recA	12	dnaK	7
ylqc	12	alaS	6
alaS	9	tig	6
tig	9	trpS	6
greA	8	ompA	6
groEL	8	rpoB	5
rpoB	7	groEL	5
trpS	7	rpoC	5
fusA	7	gatB	5
rpoC	7	pcnB	5
gatB	6	ribA	5
rpoA	6	CTL0137	4
foIP	6	rpoA	4
CTL0137	6	rpsA	4

Repeat MS experiments show co-precipitation of various ribosomal proteins along with subunits of the RNA polymerase. Using the above experiment as a framework, we performed two more MS experiments in order to control for variance. Table 5.2 provides a comprehensive list of 40 genes whose protein products consistently ranked very high in peptide counts across these three MS experiments. We recorded consistent co-precipitation of all three subunits of the RNA polymerase (rpoA, rpoB, and rpoC) along with some ribosomal proteins (such as tufA and fusA). As a comparison, data about the most abundant proteins found in *C. trachomatis* RBs and EBs from a recent proteomics study performed by Skipp et al. is shown alongside (Table 5.2) [29].

Table 5.2. Proteins consistently co-precipitated with GrgA from C. trachomatis in immunoprecipitation experiments using the anti-His antibody. GrgA and subunits of the RNA polymerase are denoted in green.

Rank	Gene Name	Known Function of Protein	Functional Category
1	NHGrgA	Transcription Factor	Transcription
2	dnaK	Chaperone	Protein Folding
3	tufA	Translation Elongation Factor	Translation
4	alaS	tRNA Ligase	Translation
5	rpoB	RNA Polymerase Subunit (β)	Transcription
6	fusA	Translation Elongation Factor	Translation
7	greA	Transcription Elongation Factor	Transcription
8	groEL	Chaperone	Protein Folding
9	rpoC	RNA Polymerase Subunit (β')	Transcription
10	ompA	Outer Membrane Protein	Membrane Protein
11	tsf	Translation Elongation Factor	Translation
12	tig	Chaperone	Protein Folding
13	gatB	Amidotransferase	Translation
14	rpsA	Ribosomal Protein	Translation
15	uvrD	DNA Helicase	DNA Replication
16	CTL0137	Unknown / Likely DNA Repair	DNA Replication
17	recA	Homologous Recombination	DNA Replication
18	gyrB	DNA Gyrase	DNA Replication
19	foIP	Folic Acid Synthesis	Metabolism
20	clpB	Chaperone	Protein Folding
21	infB	Translation Initiation Factor	Translation
22	gatA	Amidotransferase	Translation
23	cafE	Ribonuclease	RNA Binding
24	ileS	tRNA Ligase	Translation
25	rpsB	Ribosomal Protein	Translation
26	trpS	tRNA Ligase	Translation
27	glyQ	tRNA Ligase	Translation
28	ylqc	Unknown	Unknown
29	ahpC	Thioredoxin Peroxidase	Metabolism
30	nrdA	Ribonucleoside Reductase	Metabolism
31	dnaJ	Chaperone	Protein Folding
32	ribA	GTP Cyclohydrase	Metabolism
33	rpoA	RNA Polymerase Subunit (α)	Transcription
34	CTL0402	Unknown	Unknown
35	mac	Unknown	Unknown
36	pqqc	Host Cell Apoptosis	Effector Protein
37	CTL0684	Unknown	Unknown
38	nusA	Unknown	Transcription
39	pcnB	polyA Polymerase	RNA Binding
40	gyrA	DNA Gyrase	DNA Replication

Table 5.3. Most abundant proteins in RBs and EBs as detected by Skipp et al. [29] in a proteomics study of C. trachomatis. GrgA (CTL0766) and subunits of the RNA polymerase are denoted in green.

Rank	Gene Name (RBs)	Functional Category	Gene Name (EBs)	Functional Category
1	tufA	Translation	ompA	Membrane Protein
2	ompA	Membrane Protein	tufA	Translation
3	mip	Effector Protein	dnaK	Protein Folding
4	groEL	Protein Folding	hsp60_1	Protein Folding
5	omcB	Membrane Protein	mip	Effector Protein
6	CTL0887	Effector Protein	CTL0847	Effector Protein
7	dnaK	Protein Folding	rplL	Translation
8	CTL0476	Unknown	CTL0887	Effector Protein
9	CTL0323	Unknown	CTL0874	Metabolism
10	CTL0033	Unknown	acpP	Metabolism
11	CTL0847	Effector Protein	tsf	Translation
12	CTL0321	Unknown	eno	Metabolism
13	htrA	Unknown	omcB	Membrane Protein
14	pmpD	Membrane Protein	groES	Protein Folding
15	pmpG	Membrane Protein	ihfA	Unknown
16	rplL	Translation	fusA	Translation
17	fusA	Translation	CTL0512	Unknown
18	groES	Protein Folding	ahpC	Metabolism
19	CTL0255	Unknown	CTL0158	Unknown
20	sctJ	Unknown	htrA	Unknown
21	ahpC	Metabolism	rplA	Translation
22	eno	Metabolism	CTL0323	Unknown
23	acpP	Metabolism	rpoA	Transcription
24	rpoA	Transcription	rpsA	Translation
25	ompH	Membrane Protein	pmpD	Membrane Protein
26	CTL0874	Metabolism	grgA	Transcription
27	ompB	Membrane Protein	CTL0322	Unknown
28	tsf	Translation	CTL0033	Unknown
29	ptr	Unknown	rpoB	Transcription
30	gatC	Translation	ompH	Membrane Protein
31	CTL0512	Unknown	rpsB	Translation
32	rpsA	Translation	dnaJ	Protein Folding
33	rpoB	Transcription	CTL0132	Unknown
34	rpoC	Transcription	rpoC	Transcription
35	rpsB	Translation	tig	Protein Folding
36	CTL0158	Unknown	CTL0028	Unknown
37	dnaJ	Protein Folding	gatC	Translation
38	CTL0505	Unknown	recA	DNA Replication
39	pmpB	Membrane Protein	CTL0800	Unknown
40	tal	Unknown	rpsG	Translation

Immunoprecipitation under different conditions to remove nonspecific binding of some proteins did not significantly alter the results. While the presence of the three subunits of the RNA polymerase along with some transcription initiation factors such as *infB* in these immunoprecipitation results was not surprising considering that we know GrgA binds the RNA polymerase, we were alarmed to find that 12 out of the 40 proteins co-precipitated along with GrgA were either ribosomal proteins or directly involved in translation. In order to ensure that there was no indirect binding taking place between ribosomal proteins and GrgA through the presence of either RNA or DNA, we performed the immunoprecipitation under three different conditions. In the first experiment, after immunoprecipitation, we treated our samples with either DNase or RNase and performed washes subsequently to remove RNA and DNA carry over. In the second experiment, we treated *C. trachomatis* samples with 30 minutes of Rifampin treatment after induction and before cell lysis and immunoprecipitation. Since Rifampin inhibits transcription in *C. trachomatis*, treatment with Rifampin would block all nascent RNA production. In the third and last experiment, we decided to transform *C. trachomatis* with a mutant form of His-GrgA (Δ138-165) that is unable to bind DNA, and performed immunoprecipitation as before. Our findings from these three experiments indicate that the list of proteins that co-precipitate along with GrgA did not significantly change from normal conditions upon any of these treatments. Table 5.3 provides a list of 40 genes whose protein products in MS performed during these experiments.

Table 5.4. Proteins co-precipitated with GrgA from C. trachomatis under different immunoprecipitation conditions. GrgA and subunits of the RNA polymerase are denoted in green.

Plasmid Type	Full Length NH-GrgA				NH-GrgAΔ138-165
Rank	Control Treatment	RNase Treatment	DNase Treatment	Rifampin Treatment	Control Treatment
1	NHGrgA	NHGrgA	NHGrgA	NHGrgA	NHGrgA
2	dnaK	dnaK	dnaK	ompA	dnaK
3	tufA	ompA	ompA	ahpC	tufA
4	alaS	rpoB	fusA	tufA	ompA
5	rpoB	rpoC	rpoC	tig	groEL
6	fusA	alaS	rpoB	tsf	fusA
7	greA	tufA	tufA	rpoA	alaS
8	groEL	fusA	alaS	sodM	tsf
9	rpoC	rpsA	greA	alaS	uvrD
10	ompA	groEL	rpsA	folP	gatB
11	tsf	greA	gatB	ribA	tig
12	tig	uvrD	groEL	rplC	dnaJ
13	gatB	tig	tsf	rplY	gatA
14	rpsA	gatB	infB	rplD	greA
15	uvrD	CTL0137	uvrD	groEL	clpB
16	CTL0137	infB	tig	rpsC	ileS
17	recA	rpsB	CTL0137	trpS	CTL0684
18	gyrB	clpB	rpsB	rpsE	devB
19	foIP	tsf	gatA	pyrH	rpoB
20	clpB	nrdA	dnaJ	CTL0132	gatA
21	infB	gatA	ribA	dapA	rpsA
22	gatA	ribA	foIP	rpsG	rpoC
23	cafE	foIP	glyQ	recA	glyQ
24	ileS	glyQ	recA	gatA	cafE
25	rpsB	dnaJ	nrdA	CTL0322	recA
26	trpS	gyrB	dnaN	CTL0408	rpsC
27	glyQ	mac	clpB	rpsA	ileS
28	ylqc	pqqc	CTL0684	CTL0137	secA
29	ahpC	nusA	ahpC	dcd	tal
30	nrdA	ahpC	ileS	greA	lpxD
31	dnaJ	ileS	rpoA	CTL0321	foIP
32	ribA	recA	nusA	rplX	ahpC
33	rpoA	CTL0402	CTL0299	gatB	rpsB
34	CTL0402	dnaN	gyrB	rplV	glmS
35	mac	CTL0684	CTL0402	dnaJ	mip
36	pqqc	rpoA	gyrA	gyrA	rpsA
37	CTL0684	rplD	mac	CTL0887	CTL0137
38	nusA	trpS	rpsC	dnaK	nusA
39	pcnB	fabF	ispH	rplS	ispH
40	gyrA	gyrA	leuS	rpsL	nusA

DISCUSSION

In this chapter, we have detailed our attempts at identifying proteins that are associated with the *Chlamydia*-specific transcription factor, GrgA, through quantitative MS. As described previously, GrgA may bind the chlamydial RNA polymerase in order to regulate transcription. Our findings in the previous chapter indicate that GrgA associates with at least two subunits of the RNA polymerase (Table 4.5) and the two major σ factors found in *C. trachomatis* (Table 4.1). Considering this, the logical next step in the process of characterizing GrgA was to identify other proteins in *C. trachomatis* that associate with GrgA, either through direct or indirect interaction with it.

However, in spite of the fact that proteomic studies performed by Skipp et al. show that GrgA is one of the 40 most abundant proteins present in chlamydial EBs (Table 5.3), we reasoned that endogenously produced GrgA may not be suitable for our applications since certain protein-protein interactions with GrgA may be prevented by interaction between the anti-GrgA (#28) and GrgA itself, especially in cases where the binding site of the antibody is shared with another protein that associates with GrgA. As such, using an antibody against an epitope tag on the protein instead of the protein itself might be more helpful. Thus, we used the inducible gene expression system detailed by Wickstrum et al. [89] to transform *C. trachomatis* with a plasmid containing N-terminally His-tagged GrgA (NH-GrgA), and performed immunoprecipitation of His-GrgA with two GrgA-directed antibodies: a rabbit anti-GrgA antibody ("#28") and an anti-His antibody. Our initial findings using gel electrophoresis as a detection method (Fig. 5.1) indicated that both of these antibodies were capable of pulling down GrgA. However, upon performing the same experiment using MS instead of simple gel detection, we found that the anti-polyHistidine

antibody was much more suited towards our immunoprecipitation goals (Table 5.1). Furthermore, the anti-His antibody showed very little nonspecific binding when NH-GrgA was not induced from the plasmid. We therefore continued to use this antibody for the rest of our experiments.

Upon performing a set of three experiments using the same conditions, we compiled a list of genes whose protein products were consistently co-precipitated along with NH-GrgA (Table 5.2). Interestingly, the protein CTL0137, which is thought to be involved in DNA repair but has not been previously characterized, is also consistently enriched in our experiments along with GrgA, despite not being one of the many abundant proteins in *C. trachomatis.* This list contains both the α and β' subunits of the RNA polymerase, which is consistent with the *in vitro* bio-layer interferometry experiments described in the previous chapter (Table 4.5). Even though we have not shown any binding between GrgA and the β subunit of the RNA polymerase *in vitro*, it is not surprising to find β on this list as it is possible that, even if GrgA does not bind β directly, GrgA may have the ability to bind the entire holoenzyme as a whole, causing β to be consistently pulled down as part of a complex in immunoprecipitation experiments.

While it may seem initially startling, considering my findings in the previous chapter, that neither of the chlamydial σ factors are on the list in Table 5.2, this finding is not entirely unanticipated since both σ factors are known to be present in very low abundance in *C. trachomatis,* as confirmed by their absence from the list in Table 5.3. It should be noted, in fact, that both of the aforementioned research groups that performed quantitative proteomics have failed to detect σ^{28} to any extent despite covering over 60%

of the proteome in their respective studies. Thus, we theorize that GrgA-σ^{28} and GrgA-σ^{66} interactions *in vivo* are likely very transient in nature and not detectable by this method.

Upon analysis of other proteins on our list, we were surprised to learn that many translational factors (such as *tufA* and *fusA*, both of which are involved in translation elongation) and some protein folding chaperones co-precipitated with NH-GrgA (Table 5.2) as we have no previous evidence to indicate that GrgA is involved in translation, either directly or indirectly. Considering these results, one cause of concern is the use of chemical crosslinkers in our experiments. Since protein-protein interactions are often weak interactions and, as such, transient in nature, it is necessary to add crosslinkers such as DSP and DTME to cells to maintain these interactions and get a live "snapshot" of the processes inside cells. However, by virtue of the fact that GrgA can bind the RNA polymerase and DNA, it is theoretically possible to pulldown both DNA and nascent RNA from *C. trachomatis* along with GrgA. From there, ribosomal proteins and translational factors could be co-precipitated with GrgA if they are still bound to the RNA that is being translated into a nascent polypeptide.

In order to test this theory, we performed further experiments using three slightly modified conditions and compared the results from these experiments with those prior obtained above. At the outset, we treated our immunoprecipitated samples with DNase I and RNase A in order to remove genomic DNA and nascent RNA from the mix. As can be seen from the 3rd and 4th column of Table 5.3, this had no significant effect on the pulldown of ribosomal and translational proteins. It is important to note in this case that the use of DNase and RNase both caused RpoB and RpoC (β and β' respectively) to move up in ranks on the list. As a second measure towards blocking contamination via RNA, we treated our

C. trachomatis cultures with Rifampin for a short period of time before immunoprecipitation and after induction from the plasmid. Rifampin has the ability to block transcription and it specifically inhibits the DNA-directed RNA polymerase β subunit. While Rifampin treatment did block β (as can be seen from the lack of RpoB in the 5th column of Table 5.3), ribosomal proteins were still co-precipitated with GrgA in this sample and, in fact, showed more than non-treated samples. As a last measure, we constructed a mutant of NH-GrgA (Δ138-165) that cannot bind DNA (Fig. 4.5) and used it to transform *C. trachomatis*. We then overexpressed protein from this plasmid and carried out immunoprecipitation under normal conditions. As before, the use of this mutant did not alter the list significantly (6th column of Table 5.3).

While these experiments definitely prove that the presence of ribosomal and translational proteins in our immunoprecipitation products is not a result of simple variance or contamination, we are unsure about the implications of these findings as there is no other data to show interaction between GrgA and ribosomal or translational proteins. Further confounding this is the observation that a majority of the ribosomal and translational proteins co-precipitated with GrgA in this study are considered to be highly abundant according to whole-proteome analysis (Table 5.3). We are planning to, in the future, perform mass spectrometry for proteins associated with either another transcriptional regulator or one of the three chlamydial σ factors, and may have a better understanding of these results upon obtaining those data.

Regardless of whether or not GrgA binds or associates with ribosomal and translational proteins, it is evident from performing these experiments that GrgA binds the RNA polymerase subunits *in vivo*. Considering that GrgA can bind at least two of these

subunits *in vitro* too, there is a remote possibility that GrgA may have more of a role associated with the RNA polymerase than simply directing transcription. For instance, GrgA may function as a *de facto* ω factor in *C. trachomatis* and may provide help in the formation of the RNA polymerase complex. If this is true, GrgA could have even larger implications as a target for novel therapeutic agents than we have previous described.

MATERIALS AND METHODS

Reagents: The Dulbecco's modified Eagle medium (DMEM), fetal bovine serum (FBS) and trypsin (10x stock) were purchased from Sigma Aldrich. All cell culture-associated reagents (T75 flasks, 135 cm^2 dishes, serological pipettes) were purchased from Greiner Bio-One. The pGFP::CM shuttle plasmid was a generous gift from Dr. Guangming Zhong. The anhydrotetracycline (ATC), ampicillin, DSP (Lomant's reagent, or dithiobis(succinimidyl propionate)), DTME (dithiobismaleimidoethane), PMSF (phenylmethane sulfonyl fluoride), and protease inhibitor cocktail were purchased from Sigma Aldrich. The Dynabeads Antibody Coupling Kit was purchased from Thermo Fisher. Aliquots of various purified rabbit polyclonal anti-GrgA antibodies were generous gifts from Dr. Xiaofeng Bao. The rabbit IgG, mouse anti-His monoclonal antibody (H1029), mouse IgG2a antibody were purchased from Sigma Aldrich. The Crosslinking Solution was prepared by dissolving 4 mg of DSP and 3.1 mg of DTME in 500 μL of DMSO, followed by the addition of 19.5 mL of 1x PBS to this mixture, in order to yield a total volume of 20 mL containing 1 mM each of DSP and DTME. The Quenching Solution contained 1 M of Tris-HCl (pH 8.0). The Lysis Solution consisted of 25 mM Tris-HCl (pH 7.6), 1 mM EDTA, 1% SDS, 100 ug/mL PMSF, and 100 ug/mL protease inhibitors. All mass-spectrometry was performed by Dr. Caifeng Zhao at the Peter Lobel laboratory inside the Rutgers University Proteomics Center.

Cell Lines and Growth Conditions: The mouse L929 fibroblast cell line and stocks of wild-type L2 serovar (Bu343) of *C. trachomatis* were purchased from ATCC. A clone of a *C. trachomatis* L2 strain (called CPAF-deficient-Bu343) that contains two mutations in the ORF of the *CPAF* protein was a generous gift from Dr. Raphael H.

Valdivia. All cell lines were grown in DMEM containing high glucose (4.5 g/L), 110 mg sodium pyruvate, and 5% FBS in a CO_2 incubator at 37 °C.

Identification of Antibodies for Immunoprecipitation Consideration: A total of 35 different antibody options were considered for immunoprecipitation. Two out of the thirty-five antibodies were then isolated for this project based on immunostaining experiments performed by Mr. Alec Weber: rabbit anti-GrgA #28 and mouse anti-polyHistidine antibodies. Two other antibodies (rabbit IgG and mouse IgG2a) were also used as control.

Conjugation of anti-His Antibody to Dynabeads: The mouse anti-His monoclonal antibody (H1029, Sigma Aldrich) was conjugated to Dynabeads as per original protocol (or as described earlier during conjugation of the mouse anti-MOMP L2-1-5 monoclonal antibody to Dynabeads). A total of 200 µg of purified antibody was conjugated to 40 mg of Dynabeads for a high-efficiency coupling.

Plasmid Construction for Overexpression of His-GrgA: Transformation of CPAF-deficient-Bu343 was carried out by Dr. Wurihan Wurihan as per protocol [89] with a His-GrgA sequence inserted in place of the GFP sequence in pGFP::CM plasmid. As a control, the original pGFP::CM plasmid was transformed into CPAF-deficient-Bu343. Transformation efficiency and overexpression levels of His-GrgA were determined by Western blot with anti-His antibody. After isolation of efficient clones for both His-GrgA- and control vector-transformed bacteria from several passages, several T150 flasks of L929 cells were infected with each clone. These flasks were then harvested at 36 h post-infection, and all stocks were stored at -80 °C.

Isolation of Chlamydial Cell Extract and Immunoprecipitation: Multiple 135 cm^2 dishes were seeded with L929 cells and infected at 90% confluency with stocks of either the His-GrgA-transformed CPAF-deficient-Bu343 or the control-vector-transformed CPAF-deficient-Bu343. As an additional measure, 5 ug/mL ampicillin was added to the media of each dish at the time of infection in order to select for the plasmid-carrying bacteria. At 24 h post-infection, protein expression from the plasmid was induced by adding 3 ng/mL of ATC into the media of each plate and incubating for 3 hours at 37 °C. Induction efficiency was ascertained by checking RFP (for the His-GrgA-transformed bacteria) or GFP (for the control vector-transformed bacteria) levels under a fluorescent microscope at the end of the induction period. After 3 hours of induction, all medium was removed from the dishes and the cells were washed twice with ice-cold 1x PBS. After the second wash, 10 mL of the Crosslinking Solution was added to each dish, and the dishes were incubated at 4 °C. After 15 minutes, the Crosslinking Solution was removed from the dishes, and 10 mL of the Quenching Solution was added to each dish. The dishes were left on a shaker for 15 minutes on ice before all the Quenching Solution was removed from each dish. The cells were then washed three times with ice-cold 1x PBS. After the final wash, all PBS was completely removed, and the cells were lysed with the addition of 500 μL of the Lysis Solution to each dish. The cells were collected using a cell scraper into a microfuge tube, and sonicated on ice at 35% amplitude (5 seconds ON, 5 seconds OFF, 1 minute) to break open the RBs and EBs. After a high-speed spin (14000 RPM) for 20 minutes to pellet all cell debris, the supernatant was removed to a fresh tube and incubated with anti-His-coupled Dynabeads (pre-equilibriated to the Lysis Buffer) for 2 hours. After 2 hours, the Dynabeads were collected using a magnet, and the pass-through was removed.

The Dynabeads were then subject to multiple five washes with the Lysis Buffer, followed by a wash with 1x PBS. All proteins were eluted from the Dynabeads using 4x SDS Sample Laemmli Buffer, and resolved via an 8% gel. The gel was then subject to silver staining, or in the case of MS, subject to Coomassie-Blue staining. For MS experiments, samples were cut from the gel, shortened to 1 mm pieces, and collected into a tube. The tubes were then handed to Dr. Caifeng Zhao for trypsinization and eventual mass-spectrometry.

CONCLUDING REMARKS

The number of reported chlamydial infections in the US has been steadily increasing since the start of the century and is likely to approach a prevalence of 1% in the next several years [90]. While this is generally thought to be the result of advances in electronic reporting and screening technology in developed countries such as the US, it does not rule out the possibility that the prevalence of chlamydial infections could be increasing over time. Although health maintenance screening rates in the US show a pattern of general increase in the last few years from 23% in 2001 to 47% in 2015 [90], the fact that these rates can change based on whether or not screening is supported in cost by common medical insurance plans, as has been seen in recent years, makes asymptomatic infections, such as those caused by *C. trachomatis,* a matter of wide concern. Fortunately, research on *C. trachomatis* in recent years has considerably broadened our understanding of the organism, and provided plenty of research ideas to explore novel therapeutic agents against *C. trachomatis*.

Our findings in this report, split across five chapters, may have insights and applications for researchers working with either *C. trachomatis* or other bacterial species. In summary, our findings provide two broad conclusions for the *Chlamydia* research community: (i) that different species, even ones that share significant homology with each other, can demonstrate differential growth rates under similar culture conditions, and that pre-screening of any sera or media is a must at the species level rather than at the genus level; and (ii) that small-scale production of contaminant-free antibody using a specialized bioreactor such as the CELLine flask is very effective and preferable to ascites production in mice.

In addition to this, our findings also provide three straightforward conclusions about the physiology of chlamydia: (i) that the outer membrane complex of *C. trachomatis*, previously thought to be very rigid and resistant to breakdown, can be disrupted by natural organic acids such as the lactic acid produced by vaginal *Lactobacilli*, and that this inherent mechanism for defense could be harnessed towards preventing *C. trachomatis* infections in women; (ii) that the developmental cycle of all chlamydial species is temporally regulated, and that this process is likely influenced in large part by the interaction between the transcription factor, GrgA, and parts of the chlamydial RNA polymerase holoenzyme; (iii) and that GrgA is likely essential for chlamydial growth and therefore an excellent target for the development of new therapeutic antichlamydials. Indeed, concurrent research in our laboratory indicates that GrgA may be one of four possible targets for a class of novel antichlamydials, benzylidine acylhydrazides, that are highly selective.

APPENDICES

BIBLIOGRAPHY

1.	Newman, L., et al., *Global Estimates of the Prevalence and Incidence of Four Curable Sexually Transmitted Infections in 2012 Based on Systematic Review and Global Reporting.* PLoS One, 2015. **10**(12): p. e0143304.
2.	*Notifiable Diseases and Mortality Tables.* MMWR Morb Mortal Wkly Rep, 2016. **65**(3): p. ND-38.
3.	*Morbidity and Mortality Weekly Report.* Center of Disease Control, 2014. **63**(38).
4.	Stamm, W.E., *Chlamydia trachomatis infections: progress and problems.* J Infect Dis, 1999. **179 Suppl 2**: p. S380-3.
5.	Resnikoff, S., et al., *Global data on visual impairment in the year 2002.* Bull World Health Organ, 2004. **82**(11): p. 844-51.
6.	Malhotra, M., et al., *Genital Chlamydia trachomatis: an update.* Indian J Med Res, 2013. **138**(3): p. 303-16.
7.	Das, S., C. Sabin, and S. Allan, *Higher vaginal pH is associated with Chlamydia trachomatis infection in women: a prospective case-controlled study.* Int J STD AIDS, 2005. **16**(4): p. 290-3.
8.	Das, S. and S. Allan, *Higher vaginal pH is associated with Neisseria gonorrhoeae and Chlamydia trachomatis infection in a predominantly white population.* Sex Transm Dis, 2006. **33**(8): p. 527-8.
9.	Potroz, M.G. and N.J. Cho, *Natural products for the treatment of trachoma and Chlamydia trachomatis.* Molecules, 2015. **20**(3): p. 4180-203.
10.	Taylor, B.D. and C.L. Haggerty, *Management of Chlamydia trachomatis genital tract infection: screening and treatment challenges.* Infect Drug Resist, 2011. **4**: p. 19-29.
11.	Karska-Wysocki, B., M. Bazo, and W. Smoragiewicz, *Antibacterial activity of Lactobacillus acidophilus and Lactobacillus casei against methicillin-resistant Staphylococcus aureus (MRSA).* Microbiol Res, 2010. **165**(8): p. 674-86.
12.	Gupta, K., et al., *Inverse association of H2O2-producing lactobacilli and vaginal Escherichia coli colonization in women with recurrent urinary tract infections.* J Infect Dis, 1998. **178**(2): p. 446-50.
13.	Gong, Z., et al., *Lactobacilli inactivate Chlamydia trachomatis through lactic acid but not H2O2.* PLoS One, 2014. **9**(9): p. e107758.
14.	Hoffman, M.K., et al., *A Comparison of Colorimetric Assessment of Vaginal pH with Nugent Score for the Detection of Bacterial Vaginosis.* Infectious Diseases in Obstretrics and Gynecology, 2017. **2017**.
15.	Liu, X., et al., *Identification of Chlamydia trachomatis outer membrane complex proteins by differential proteomics.* J Bacteriol, 2010. **192**(11): p. 2852-60.
16.	Doron, S.I., P.L. Hibberd, and S.L. Gorbach, *Probiotics for prevention of antibiotic-associated diarrhea.* J Clin Gastroenterol, 2008. **42 Suppl 2**: p. S58-63.
17.	Hempel, S., et al., *Probiotics for the prevention and treatment of antibiotic-associated diarrhea: a systematic review and meta-analysis.* JAMA, 2012. **307**(18): p. 1959-69.
18.	Nagpal, R., et al., *Probiotics, their health benefits and applications for developing healthier foods: a review.* FEMS Microbiol Lett, 2012. **334**(1): p. 1-15.
19.	Hibberd, P.L., et al., *No evidence of harms of probiotic Lactobacillus rhamnosus GG ATCC 53103 in healthy elderly-a phase I open label study to assess safety, tolerability and cytokine responses.* PLoS One, 2014. **9**(12): p. e113456.
20.	Pridmore, R.D., et al., *Hydrogen peroxide production by Lactobacillus johnsonii NCC 533 and its role in anti-Salmonella activity.* FEMS Microbiol Lett, 2008. **283**(2): p. 210-5.
21.	Kalyoussef, S., et al., *Lactobacillus proteins are associated with the bactericidal activity against E. coli of female genital tract secretions.* PLoS One, 2012. **7**(11): p. e49506.
22.	Jayashree, S., et al., *Anti-adhesion Property of the Potential Probiotic Strain Lactobacillus fermentum 8711 Against Methicillin-Resistant Staphylococcus aureus (MRSA).* Front Microbiol, 2018. **9**: p. 411.
23.	Mastromarino, P., et al., *Effects of vaginal lactobacilli in Chlamydia trachomatis infection.* Int J Med Microbiol, 2014. **304**(5-6): p. 654-61.

24. Nardini, P., et al., *Lactobacillus crispatus inhibits the infectivity of Chlamydia trachomatis elementary bodies, in vitro study.* Sci Rep, 2016. **6**: p. 29024.

25. Caldwell, H.D., J. Kromhout, and J. Schachter, *Purification and partial characterization of the major outer membrane protein of Chlamydia trachomatis.* Infect Immun, 1981. **31**(3): p. 1161-76.

26. Tang, F.F., et al., *Studies on the etiology of trachoma with special reference to isolation of the virus in chick embryo.* Chin Med J, 1957. **75**(6): p. 429-47.

27. Banhart, S., et al., *Chlamydia trachomatis and its interaction with the cellular retromer.* Int J Med Microbiol, 2017.

28. Saka, H.A., et al., *Quantitative proteomics reveals metabolic and pathogenic properties of Chlamydia trachomatis developmental forms.* Mol Microbiol, 2011. **82**(5): p. 1185-203.

29. Skipp, P.J., et al., *Quantitative Proteomics of the Infectious and Replicative Forms of Chlamydia trachomatis.* PLoS One, 2016. **11**(2): p. e0149011.

30. Albrecht, M., et al., *Deep sequencing-based discovery of the Chlamydia trachomatis transcriptome.* Nucleic Acids Res, 2010. **38**(3): p. 868-77.

31. Humphrys, M.S., et al., *Simultaneous transcriptional profiling of bacteria and their host cells.* PLoS One, 2013. **8**(12): p. e80597.

32. Howard, L., N.S. Orenstein, and N.W. King, *Purification on renografin density gradients of Chlamydia trachomatis grown in the yolk sac of eggs.* Appl Microbiol, 1974. **27**(1): p. 102-6.

33. Mukhopadhyay, S., et al., *Detailed protocol for purification of Chlamydia pneumoniae elementary bodies.* J Clin Microbiol, 2004. **42**(7): p. 3288-90.

34. Bose, S.K. and R.G. Paul, *Purification of Chlamydia trachomatis lymphogranuloma venereum elementary bodies and their interaction with HeLa cells.* J Gen Microbiol, 1982. **128**(6): p. 1371-9.

35. Newhall, W.J., B. Batteiger, and R.B. Jones, *Analysis of the human serological response to proteins of Chlamydia trachomatis.* Infect Immun, 1982. **38**(3): p. 1181-9.

36. Putman, T.E., et al., *Culture-independent sequence analysis of Chlamydia trachomatis in urogenital specimens identifies regions of recombination and in-patient sequence mutations.* Microbiology, 2013. **159**(Pt 10): p. 2109-17.

37. Stone, S.S., J.M. Patterson, and B.L. Deyoe, *Extraction, separation, and partial characterization of Brucella abortus antigens.* Am J Vet Res, 1982. **43**(1): p. 149-53.

38. Anwari, K., et al., *A modular BAM complex in the outer membrane of the alpha-proteobacterium Caulobacter crescentus.* PLoS One, 2010. **5**(1): p. e8619.

39. Yaciuk, P., *Co-immunoprecipitation of protein complexes.* Methods Mol Med, 2007. **131**: p. 103-11.

40. Iqbal, H., D.R. Akins, and M.R. Kenedy, *Co-immunoprecipitation for Identifying Protein-Protein Interactions in Borrelia burgdorferi.* Methods Mol Biol, 2018. **1690**: p. 47-55.

41. Verhelst, J., D. De Vlieger, and X. Saelens, *Co-immunoprecipitation of the Mouse Mx1 Protein with the Influenza A Virus Nucleoprotein.* J Vis Exp, 2015(98).

42. Lin, J.S. and E.M. Lai, *Protein-Protein Interactions: Co-Immunoprecipitation.* Methods Mol Biol, 2017. **1615**: p. 211-219.

43. Lara, O., et al., *Enrichment of rare cancer cells through depletion of normal cells using density and flow-through, immunomagnetic cell separation.* Exp Hematol, 2004. **32**(10): p. 891-904.

44. Schmitz, B., et al., *Magnetic activated cell sorting (MACS)--a new immunomagnetic method for megakaryocytic cell isolation: comparison of different separation techniques.* Eur J Haematol, 1994. **52**(5): p. 267-75.

45. Clarke, C. and S. Davies, *Immunomagnetic cell separation.* Methods Mol Med, 2001. **58**: p. 17-23.

46. Bhuvanendran Nair Gourikutty, S., C.P. Chang, and P.D. Puiu, *Microfluidic immunomagnetic cell separation from whole blood.* J Chromatogr B Analyt Technol Biomed Life Sci, 2016. **1011**: p. 77-88.

47. Blake, J.M., et al., *Improved immunomagnetic enrichment of CD34(+) cells from umbilical cord blood using the CliniMACS cell separation system.* Cytotherapy, 2012. **14**(7): p. 818-22.

48. Yakub, G.P. and K.L. Stadterman-Knauer, *Immunomagnetic separation of pathogenic organisms from environmental matrices.* Methods Mol Biol, 2004. **268**: p. 189-97.

49. Kim, D.K., et al., *Scalable Production of a Multifunctional Protein (TSG-6) That Aggregates with Itself and the CHO Cells That Synthesize It.* PLoS One, 2016. **11**(1): p. e0147553.

50. Taylor, N.M.I., et al., *Structure of the human multidrug transporter ABCG2.* Nature, 2017. **546**(7659): p. 504-509.

51. Bruce, M.P., et al., *Dialysis-based bioreactor systems for the production of monoclonal antibodies--alternatives to ascites production in mice.* J Immunol Methods, 2002. **264**(1-2): p. 59-68.

52. Westermann, A.J., L. Barquist, and J. Vogel, *Resolving host-pathogen interactions by dual RNA-seq.* PLoS Pathog, 2017. **13**(2): p. e1006033.

53. Yao, J., et al., *Chlamydia trachomatis Relies on Autonomous Phospholipid Synthesis for Membrane Biogenesis.* J Biol Chem, 2015. **290**(31): p. 18874-88.

54. Fang, C.Y., et al., *Long-term growth comparison studies of FBS and FBS alternatives in six head and neck cell lines.* PLoS One, 2017. **12**(6): p. e0178960.

55. Abdelrahman, Y.M. and R.J. Belland, *The chlamydial developmental cycle.* FEMS Microbiol Rev, 2005. **29**(5): p. 949-59.

56. Anderson, I.E. and T.A. Baxter, *Chlamydia psittaci: inclusion morphology in cell culture and virulence in mice of ovine isolates.* Vet Rec, 1986. **119**(18): p. 453-4.

57. Elwell, C., K. Mirrashidi, and J. Engel, *Chlamydia cell biology and pathogenesis.* Nat Rev Microbiol, 2016. **14**(6): p. 385-400.

58. Lepinay, A., et al., *[Study with electron microscopy of the development and morphology of Chlamydia psittaci in mouse macrophages].* Ann Inst Pasteur (Paris), 1970. **119**(2): p. 222-31.

59. Miyashita, N., Y. Kanamoto, and A. Matsumoto, *The morphology of Chlamydia pneumoniae.* J Med Microbiol, 1993. **38**(6): p. 418-25.

60. Stirling, P. and S. Richmond, *The developmental cycle of Chlamydia trachomatis in McCoy cells treated with cytochalasin B.* J Gen Microbiol, 1977. **100**(1): p. 31-42.

61. Yamazaki, T., *[Morphology and immunotyping of AC-43 strain of Chlamydia pneumoniae isolated from a Japanese child].* Kansenshogaku Zasshi, 1992. **66**(5): p. 632-6.

62. Mathews, S.A., K.M. Volp, and P. Timms, *Development of a quantitative gene expression assay for Chlamydia trachomatis identified temporal expression of sigma factors.* FEBS Lett, 1999. **458**(3): p. 354-8.

63. Nicholson, T.L., et al., *Global stage-specific gene regulation during the developmental cycle of Chlamydia trachomatis.* J Bacteriol, 2003. **185**(10): p. 3179-89.

64. Shaw, E.I., et al., *Three temporal classes of gene expression during the Chlamydia trachomatis developmental cycle.* Mol Microbiol, 2000. **37**(4): p. 913-25.

65. Slepenkin, A., et al., *Temporal expression of type III secretion genes of Chlamydia pneumoniae.* Infect Immun, 2003. **71**(5): p. 2555-62.

66. Belland, R.J., et al., *Genomic transcriptional profiling of the developmental cycle of Chlamydia trachomatis.* Proc Natl Acad Sci U S A, 2003. **100**(14): p. 8478-83.

67. Ishihama, A., *Subunit of assembly of Escherichia coli RNA polymerase.* Adv Biophys, 1981. **14**: p. 1-35.

68. Gu, L., et al., *Chlamydia trachomatis RNA polymerase alpha subunit: sequence and structural analysis.* J Bacteriol, 1995. **177**(9): p. 2594-601.

69. Douglas, A.L. and T.P. Hatch, *Expression of the transcripts of the sigma factors and putative sigma factor regulators of Chlamydia trachomatis L2.* Gene, 2000. **247**(1-2): p. 209-14.

70. Hua, Z., et al., *Mutagenesis of region 4 of sigma 28 from Chlamydia trachomatis defines determinants for protein-protein and protein-DNA interactions.* J Bacteriol, 2009. **191**(2): p. 651-60.

71. Koehler, J.E., et al., *Chlamydia trachomatis RNA polymerase major sigma subunit. Sequence and structural comparison of conserved and unique regions with Escherichia coli sigma 70 and Bacillus subtilis sigma 43.* J Biol Chem, 1990. **265**(22): p. 13206-14.

72. Mathews, S.A. and P. Timms, *Identification and mapping of sigma-54 promoters in Chlamydia trachomatis.* J Bacteriol, 2000. **182**(21): p. 6239-42.

73. Fahr, M.J., et al., *Characterization of late gene promoters of Chlamydia trachomatis.* J Bacteriol, 1995. **177**(15): p. 4252-60.

74. Grech, B., S. Mathews, and P. Timms, *Phylogenetic comparison of the known Chlamydia trachomatis sigma(66) promoters across to Chlamydia pneumoniae and Chlamydia caviae identifies seven poorly conserved promoters.* Res Microbiol, 2008. **159**(7-8): p. 550-6.

75.   Cong, Y., et al., *Quantifying promoter activity during the developmental cycle of Chlamydia trachomatis.* Sci Rep, 2016. **6**: p. 27244.

76.   Shen, L., et al., *Selective promoter recognition by chlamydial sigma28 holoenzyme.* J Bacteriol, 2006. **188**(21): p. 7364-77.

77.   Shen, L., M. Li, and Y.X. Zhang, *Chlamydia trachomatis sigma28 recognizes the fliC promoter of Escherichia coli and responds to heat shock in chlamydiae.* Microbiology, 2004. **150**(Pt 1): p. 205-15.

78.   Yu, H.H. and M. Tan, *Sigma28 RNA polymerase regulates hctB, a late developmental gene in Chlamydia.* Mol Microbiol, 2003. **50**(2): p. 577-84.

79.   Bao, X., B.E. Nickels, and H. Fan, *Chlamydia trachomatis protein GrgA activates transcription by contacting the nonconserved region of sigma66.* Proc Natl Acad Sci U S A, 2012. **109**(42): p. 16870-5.

80.   Fisher, D.J., N.E. Adams, and A.T. Maurelli, *Phosphoproteomic analysis of the Chlamydia caviae elementary body and reticulate body forms.* Microbiology, 2015. **161**(8): p. 1648-58.

81.   Grieshaber, N.A., et al., *Regulation of the Chlamydia trachomatis histone H1-like protein Hc2 is IspE dependent and IhtA independent.* J Bacteriol, 2006. **188**(14): p. 5289-92.

82.   Kiselev, A.O., M.C. Skinner, and M.F. Lampe, *Analysis of pmpD expression and PmpD post-translational processing during the life cycle of Chlamydia trachomatis serovars A, D, and L2.* PLoS One, 2009. **4**(4): p. e5191.

83.   Koo, I.C., et al., *ChxR is a transcriptional activator in Chlamydia.* Proc Natl Acad Sci U S A, 2006. **103**(3): p. 750-5.

84.   Rao, X., et al., *A regulator from Chlamydia trachomatis modulates the activity of RNA polymerase through direct interaction with the beta subunit and the primary sigma subunit.* Genes Dev, 2009. **23**(15): p. 1818-29.

85.   Rosario, C.J., B.R. Hanson, and M. Tan, *The transcriptional repressor EUO regulates both subsets of Chlamydia late genes.* Mol Microbiol, 2014. **94**(4): p. 888-97.

86.   Schmidt, T.G. and A. Skerra, *The Strep-tag system for one-step purification and high-affinity detection or capturing of proteins.* Nat Protoc, 2007. **2**(6): p. 1528-35.

87.   Hooppaw, A.J. and D.J. Fisher, *A Coming of Age Story: Chlamydia in the Post-Genetic Era.* Infect Immun, 2015. **84**(3): p. 612-21.

88.   Hybiske, K., *Expanding the Molecular Toolkit for Chlamydia.* Cell Host Microbe, 2015. **18**(1): p. 11-3.

89.   Wickstrum, J., et al., *Conditional gene expression in Chlamydia trachomatis using the tet system.* PLoS One, 2013. **8**(10): p. e76743.

90.   *2016 Sexually Transmitted Diseases Surveillance.* Center of Disease Control, 2016.